Neural mechanisms of inhibitory control revealed by network analysis of structural/functional MRI data

by

FAN ZHANG

THESIS SUBMITTED IN FULFILMENT OF THE REQUIREMENTS FOR THE

PHD DEGREE

at

Graduate School of Comprehensive Human Sciences

University of Tsukuba

December 2019

Abstract of the Dissertation

The ability to voluntarily inhibit actions when it has become inappropriate or even dangerous in a certain environment is crucial for human life. Successful behavioral inhibition involves two components: proactive and reactive inhibition. The former is goal-directed, which means people need to withhold and adjust reactions for the upcoming task demands. In contrast, the latter is triggered by the stimulus. Therefore, the planned action must be canceled when a stop signal is detected. Converging evidence suggests that frontal cortical regions and basal ganglia in human brain dedicated to proactive and reactive inhibitory control. However, it is still unclear about the neural mechanisms underlying inhibitory control, and how does the information flow during proactive and reactive inhibition.

The aim of this PHD research is to investigate the brain circuits involved inhibitory control. I conducted two studies and employed one experiment. The aim of first study was to identify the regions involved in stop-signal task, clarify the role of these regions and further examine the causal relationships between these regions in proactive and reactive inhibition. I used a specific contrast to isolate the proactive inhibitory control from the reactive inhibitory control, and the regions showing

significant activations were applied to the following dynamic and anatomical analysis. The dynamic causal modeling (DCM) was used in first study for the analysis of effective connectivity between the prior selected set of brain regions. In the second study, I combined the functional magnetic resonance imaging (fMRI) and diffusion tensor imaging (DTI) method to examine the relationship between functional and structural interactions in behavioral control task. I defined the white matter tracts of interest via probabilistic tractography and used fractional anisotropy (FA) as an indicator of white matter integrity in the subsequent statistical analysis. The data-driven hierarchical clustering and microstructural correlations were combined to examine whether a specific pattern also exists in white matter tracts.

In the first study, I worked on the fMRI data and found the “longer” pathway DLPFC-caudate-IFG-SMA-STN-M1 and the “shorter” pathway IFG-SMA-STN-M1 involved in proactive and reactive inhibitory control separately. Especially, the effective connectivity from caudate to IFG was modulated by proactive inhibition, while the reactive modulation influenced on the effective connectivity from IFG to SMA.

In the second study, I applied the DTI and probabilistic fiber tractography to examine how the white matter microstructure tracts are related to response inhibition, and how the interaction between these tracts transfer the information in the brain. The

combination of data-driven hierarchical clustering and significant correlation of FA revealed the specific clusters in the fronto-basal ganglia circuits, and the certain pairs of white matter tracts with significant correlations predicted the effective pathways between DLPFC-caudate/ caudate-IFG/ IFG-SMA/ SMA-STN neural circuits for behavioral control. The results supported the previous result from the first study that focused on fMRI data analysis and examined the relationship between white matter microstructure and functional connectivity.

Taken together, the studies showed that 1) the indirect DLPFC-caudate-IFG-SMA-STN-M1 pathway is involved in the implement of proactive modulation, while the hyperdirect pathway that bypasses the striatum contributes to the reactive modulation. Especially, the effective connection from caudate to IFG was modulated by proactive inhibition, while reactive modulation acted on the effective connection from IFG to SMA. The result of dynamic causal modelling revealed that the function of IFG is more related to attention control in response inhibition, 2) the further investigation using diffusion tensor imaging (DTI) and probabilistic fiber tractography also provided the evidences in micro-structural level for the effective connectivity between DLPFC-caudate-IFG-SMA-STN neural circuits. The combined results from the hierarchical

clustering and microstructural correlation of FA predicted the effective pathway which support the previous conclusion in the first study.

Contents

Study 1 Common neural network for different functions: an investigation of proactive and reactive inhibition

Introduction

Behavioral control is a critical ability to inhibit planned response or prevent inappropriate behavior when the environment changes. It has been found as an effective behavioral marker to predict the cognitive ability (Harnishfeger & Björklund, 1994), and the impairments in response inhibition are associated with various disorders including attention deficit/hyperactivity disorder (ADHD; Barkley, 1997; Simmonds, Pekar, & Mostofsky, 2008; McLoughlin et al., 2010), Parkinson's disease as well as tourette and obsessive-compulsive patients (Mirabella et al., 2008, 2013, 2017; Mancini et al., 2018, 2019), obsessive compulsive disorder (OCD; Bannon, Gonsalvez, Croft, & Boyce, 2002) and posttraumatic stress disorder (PTSD; van Rooij, Geuze, Kennis, Rademaker, & Vink, 2014). The completion of inhibitory control involves a number of cognitive processes requiring the complex cooperation between areas in the brain. Thus, the investigation of inhibitory control, especially the interactions existing in neural

circuits, will contribute to not only the theoretical research, but also the clinical application.

1.1 Theoretical background

Successful inhibitory control involves two typically components: proactive and reactive inhibition (Braver et al., 2007; Jaffard et al., 2007; Aron, 2011; Bari and Robbins, 2013). The former acts to prepare and adjust the response in anticipation of the upcoming cue (Verbruggen and Logan, 2009; Chikazoe et al., 2009b), while the latter is cue-triggered and occurs when a stop signal is detected (Eagle et al., 2008; Chambers et al., 2009; Aron et al., 2014). Over the past decade, the neural circuits underlying reactive inhibition, which only occurs after and close to the stop signal, have been comprehensively investigated via using stop-signal task (Logan and Cowan, 1984; Logan et al., 1997). Conversely, the property of proactive inhibition that requires the consideration of goal-relevant information to adjust the motor system poses leads to the difficulty of ensuring the time of occurrence. Thus, compared to substantial research in reactive inhibition, relatively few studies focus on the neural mechanism underlying proactive inhibition. The following sections will review the related studies about the neural mechanisms and the behavioral tasks used for proactive and reactive inhibition.

1.1.1 The behavioral task used to investigate the inhibitory control

In the history of cognitive inhibition research, one of the difficulties is the inhibitory control cannot be measured directly. The majority of the behavioral control tasks evaluate the effects of inhibition by requiring participants to inhibit the irrelevant or interference information and assess the reaction time (RT) representing the cost for response behavioral inhibition as an indicative parameter (Stroop, 1935). However, although the difference between RTs indicates the degree of ability of inhibitory control, it provides little information about the neural mechanism when people inhibit the inappropriate behaviors.

A breaking point occurred when the Stop-signal task (SST) was brought up and developed by Logan et al (Lappin and Eriksen, 1966; Logan and Cowan, 1984; Logan et al., 1984). The SST provides the possibility to isolate the inhibitory process directly and investigate the underlying neural circuits for response inhibition.

The classical SST consists of frequent “go” trials and infrequent “signal” trials. Participants are required to make a response as fast as possible in “go” trials but cancel the response or start a new movement when a new signal follows the initial “go” signal in “signal” trial. The delay between the onset of initial “go” signal and “signal” signal (stop signal delay, SSD) is a parameter for determining the success rate of participants to successfully stop the planned action (Lappin and Eriksen, 1966; Logan et al., 1984).

The longer SSD predicts the decreased success rate in the performance of participants. The stop-signal reaction time (SSRT) is primarily used to estimate the effect of reactive inhibition (Bunge et al., 2002; Band et al., 2003).

The application of classical stop-signal task was successful in the study of reactive inhibition. For proactive inhibition, it requires a modified paradigm because of the difficulty in identifying the onset of occur time. The additional cues in the modified go/no-go task indicate the possibility of upcoming stop-signals, while the SSRT is modified by considering the effect of uncertainty for "go" cues (Chikazoe et al. 2009a; Jahfari et al. 2010; Swann et al. 2012; Aron et al. 2014; Cunillera et al. 2014; Verbruggen et al. 2014b; Cai et al. 2016). Recently, a paradigm comparing the reaction times (RTs) and movement times (MTs) of reaching arm movements in different contexts was applied to the investigation of deficits in proactive inhibition in healthy subjects, in Parkinson's patients, as well as in Tourette and obsessive-compulsive patients (Mirabella et al., 2008, 2013, 2017; Mancini et al., 2018, 2019).

1.1.2 Functional Magnetic Resonance Imaging and hemodynamic response

Functional Magnetic Resonance Imaging (fMRI) is one of the remarkable non-invasive technique to measure brain activity. The principle is based on the direction of angular momentum of protons, neutrons and electrons can be changed in a strong

external magnetic field. fMRI measures the neural activity indirectly by the changes in blood oxygenation level dependent (BOLD) signal that is known as hemodynamic response (HDR). The shape of HDR reflects the properties of stimulus and the underlying neural activity. Thus, people can decode the information by analyzing the pattern of neural response, which constitute the theoretical frame and basis for the conventional neuroimaging analysis.

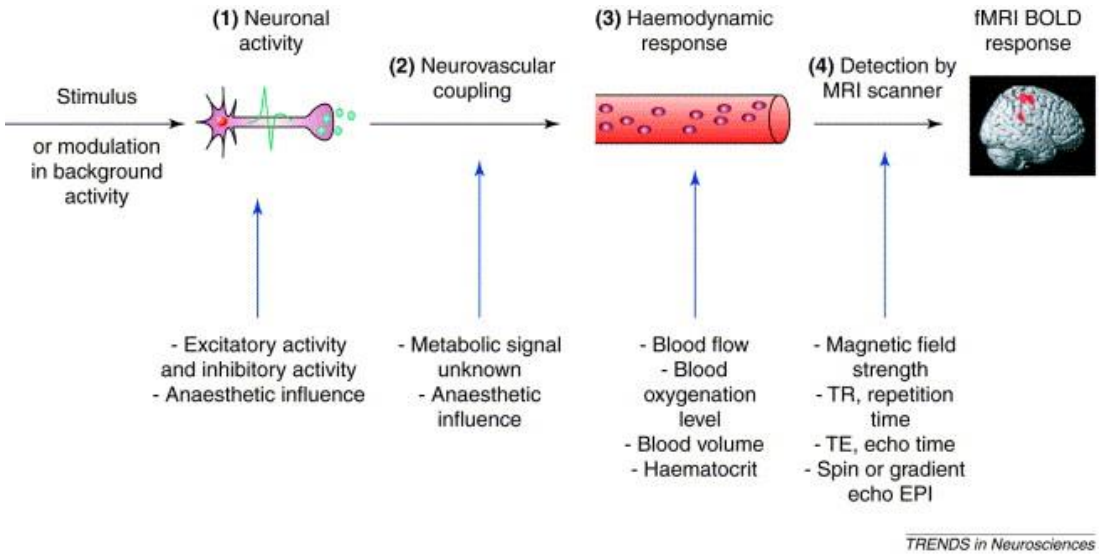

Fig.1. How does the BOLD signal be detected : (1) the neuronal response to a stimulus or background modulation; (2) the complex relationship between neuronal activity and triggering a hemodynamic response (termed neurovascular coupling); (3) the hemodynamic response itself; and (4) the way in which this response is detected by an MRI scanner. (Arthurs OJ, 2002)

1.1.3 Horse race model

The SST that participants need to selective stopping leads to the model proposed by Logan and Cowan (1984), the horse race model. In this model, the behavioral control is a race between two different neural processes: the "go" process and the "stop" process. The behavioral outcome is determined by which process first reaches the activation threshold and wins the race. If the "go" process reaches first, participants make the response. Otherwise, preparation for the response is aborted. The horse race model assumes that the rate of accumulation of each process is constant, and the only determinant factor for successful inhibition is the delay between the onset of "go" and "stop" process. Thus, another parameter was introduced based on the race model, the stop signal reaction time (SSRT). The SSRT represents the latency of the "stop" process and it can only be estimated by comparing the distribution of go RTs with SSD. The RT longer than SSRT will be captured by the stop process.

The horse race model has been widely applied in the behavioral control studies. It provides a theoretical frame to understand the neural mechanism of behavioral inhibition by investigating the race between "go" and "stop" process. However, the horse race model considering the behavioral outcoming is only the race between two hypothetical processes oversimplifies the complexity of goal-directed behavior. A successful goal-directed behavior involves the cooperation of many cognitive processes

such as attentional control and select the appropriate actions. The race model is inadequate to explain the flexible and sophisticated dynamics between neural circuits in the brain when people adapts to the changing environment.

1.1.4 Neural pathways for response inhibition

It has been suggested that the successful inhibitory control process involves the preparation and termination of response via two distinct controls: proactive and reactive control. Proactive control requires the goal-relevant information to prepare for the possible stop command, while the reactive control relies upon the detection of a new stimulus representing the stop signal.

The fMRI techniques can be used to identify the regions related to reactive inhibition. The prefrontal cortex (PFC), particularly the inferior frontal gyrus (IFG) and the presupplementary motor area (preSMA)/ supplementary motor area (SMA), are suggested to be critical for reactive inhibition (Simmonds et al., 2008; Chikazoe, 2010; Jahfari et al., 2010; Wardak, 2011; Cunillera et al., 2014; Verbruggen et al., 2014; Rae et al., 2015). An electrocorticographic study of stop-event related potentials has investigated the fronto-temporal lobes of patients with pharmacoresistant epilepsy and found the causal involvement of the premotor area (PMA), the primary cortex (M1), and Brodmann's area (BA) 9. The study showed that M1 is the destination in the frontal-

basal ganglia-thalamic network in a cognitive control task (Mattia et al., 2012). Furthermore, a substantial proportion (30%) of monkey dorsal premotor cortex (PMd) cells produced signals predicting forthcoming actions in a reaching version of the stop-signal task, which suggests that both the M1 and PMd participated in the inhibitory control task (Coxon et al., 2006; Mirabella et al., 2011; Mattia et al., 2013). These areas combine with the basal ganglia to form a network that inhibits the activation of the M1 during reactive inhibition.

In contrast, the metabolic activity associated with proactive inhibition, which can occur throughout the task, cannot be isolated based on simple neuroimaging contrasts. Previous research has indicated that parts of the reactive inhibition network including the IFG and subthalamic nucleus (STN) are also involved in proactive inhibition (Aron et al., 2014). The application of deep brain stimulation (DBS) to the bilateral STN of patients with Parkinson's led to shorter SSRT in a stop signal task (van den Wildenberg et al., 2006; Frank et al., 2007; Mirabella et al., 2012a,b), and a similar improvement in appropriate motor strategies that represent proactive inhibitory ability was also found in bilateral DBS of the STN of patients with Parkinson's (Mirabella et al., 2013). However, no improvement was found with unilateral DBS (Mancini et al.,

2019), which is opposed to the hypothesis that the right STN is critical to response inhibition (Aron and Poldrack, 2006; Aron et al., 2014).

Previous research has revealed that the basal ganglia circuits are centrally involved in behavioral control via direct (cortico-striato-nigral) and indirect (cortico-striato-pallido-subthalamonigral) pathways (Alexander et al., 1986; Albin et al., 1989; DeLong, 1990; Aron et al., 2007a, b). When a cortical signal relating to a voluntary movement is transmitted to the striatum, the activated striatum inhibits the activity of the globus pallidus internalis (GPi) via inhibitory GABAergic projections. The result leads to the disinhibition of thalamus and then to the generation of movement (direct pathway). In contrast, the activated striatum inhibits the globus pallidus externalis (GPe) via inhibitory GABAergic projections, which in turn disinhibits the activities of GPi and further inhibit the activity of the thalamus, leading to the inhibition of movement (indirect pathway).

The inhibitory effect carried out through indirect pathway acts slower than the excitatory effect executed via the direct pathway. Thus, it raises a question that how the brain stops the “go” process once it is initiated, because the slower “stop” process cannot catch up with the “go” process. Another pathway, the hyper-direct pathway, which is also involved in motion information processing answers this question (Nambu

et al., 2000, 2002; Baker et al., 2010; Dunovan et al., 2015). The hyperdirect pathway bypasses the striatum and connects the cortex and the STN directly, then activates the GPi to inhibit the activity of the thalamus in a faster way. Recently, a study related to cortical-basal ganglia networks suggested a new hypothesis of action inhibition: the action is paused via a subthalamic-nigra pathway in the preparation step and canceled through arkypallidal GABAergic projection.

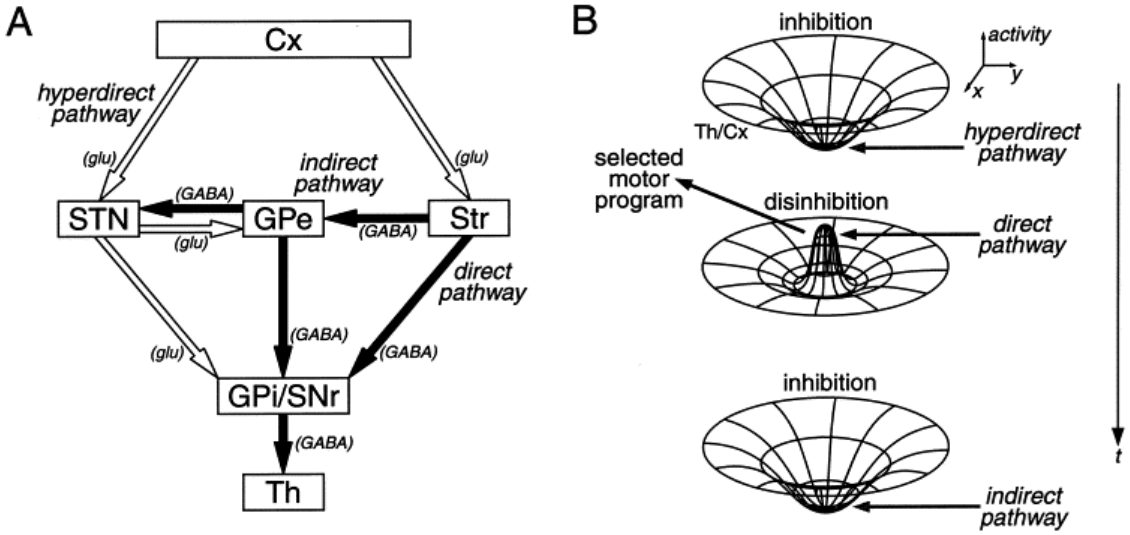

Fig. 2. Schematic diagram of the "direct"/ "indirect"/ "hyperdirect" pathway. Open and filled arrows represent excitatory glutamatergic (glu) and inhibitory GABAergic (GABA) projections, respectively. Cx, cerebral cortex; GPe, external segment of the globus pallidus; GPi, internal segment of the globus pallidus; SNr, substantia nigra pars reticulata; STN, subthalamic nucleus; Str, striatum; Th, thalamus. (Nambu et al., 2000b)

1.1.5 General linear Model (GLM)

General linear Model (GLM) is one of the most common statistical method in fMRI to model the BOLD signal and make statistical inferences about the specific areas that related to cognitive tasks. It assumes that the BOLD signal of a given voxel can be modelled as a sum of many weighted independent variables with noise (Huettel et al., 2008). The GLM equation can be expressed as the following:

$$\boldsymbol{Y} = \boldsymbol{X\beta} + \boldsymbol{\epsilon}$$

While Y is a column vector containing the BOLD signal of time-series at a given voxel. $\boldsymbol{\beta}$ is a column vector of model parameters that determines the how much weight one variable in design matrix X contributes to the model. X is a design matrix specifying the linear model to be evaluated. $\boldsymbol{\epsilon}$ is the residual error vector or noise.

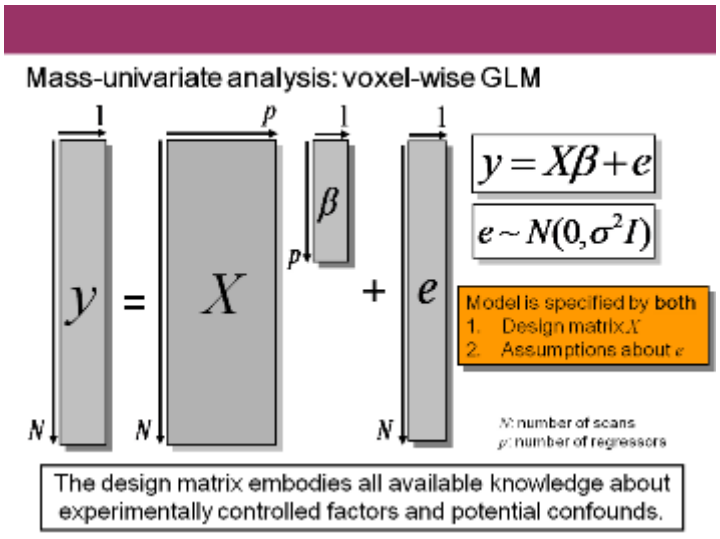

Fig. 3. Schematic diagram of GLM for SPM (from SPM course slides)

The solution from GLM equations are the beat-weights or estimated model parameters. Under the null hypothesis, the significant of voxels were evaluated based on a statistical distribution called the F-distribution (Huettel et al. 2008; Jezzard et al. 2003). The areas with significant activations were considered as regions of interest that associated with cognitive tasks.

1.1.6 Dynamic causal modeling (DCM)

The underlying neural pathways for response inhibition have been relatively clear via the traditional research of regional activation fMRI studies. However, the effective connectivity and directional relationships between these functional-related brain regions remains unclear. For example, a large number of studies have suggested that the right IFG is a critical region in response inhibition, but not much research have been conducted in the influence that other regions received from the IFG other regions during the inhibitory process. Furthermore, does these regions influence other regions directionally or reciprocally? In the cognitive task such as response inhibition, are there any crucial connections in both forms of inhibitory control?

The dynamic causal modelling (DCM) is a Bayesian framework that infers the causal structure and effective connectivity within models of neuronal response that measured by fMRI or other functional imaging methods. The principle of DCM is the

application of the inversion of generative or forward (state-space) models of observable response to infer how neuronal activity causes measurements. The model parameters and the marginal likelihood or model evidence for inferences are generally estimated by standard Variational Laplace (Friston et al., 2007) procedure, and further applied in the analysis of specific effective connections and network architecture (Daunizeau et al., 2011; Penny et al., 2004).

In brief, experimental and extrinsic input arrives at granular layer, targeting spiny stellate cells. These populations then project to superficial pyramidal cells, which project to deep pyramidal cells. In addition to this intrinsic feedforward pathway (Thomson and Bannister, 2003), there are reciprocal connections with inhibitory interneurons, modelled here with a single population. Extrinsic efferent come in two flavors. Forward connections arise from superficial pyramidal cells, while backward connections arise from deep pyramidal cells (Felleman and Van Essen, 1991; Hilgetag et al., 2000). Extrinsic forward connections provide the input to the granular layer of a higher region (with a small projection to deep pyramidal cells), while extrinsic backward connections target superficial pyramidal cells and inhibitory interneurons. Note that the recurrent (self) connections are universally inhibitory; irrespective of whether the neuronal population is excitatory or inhibitory.

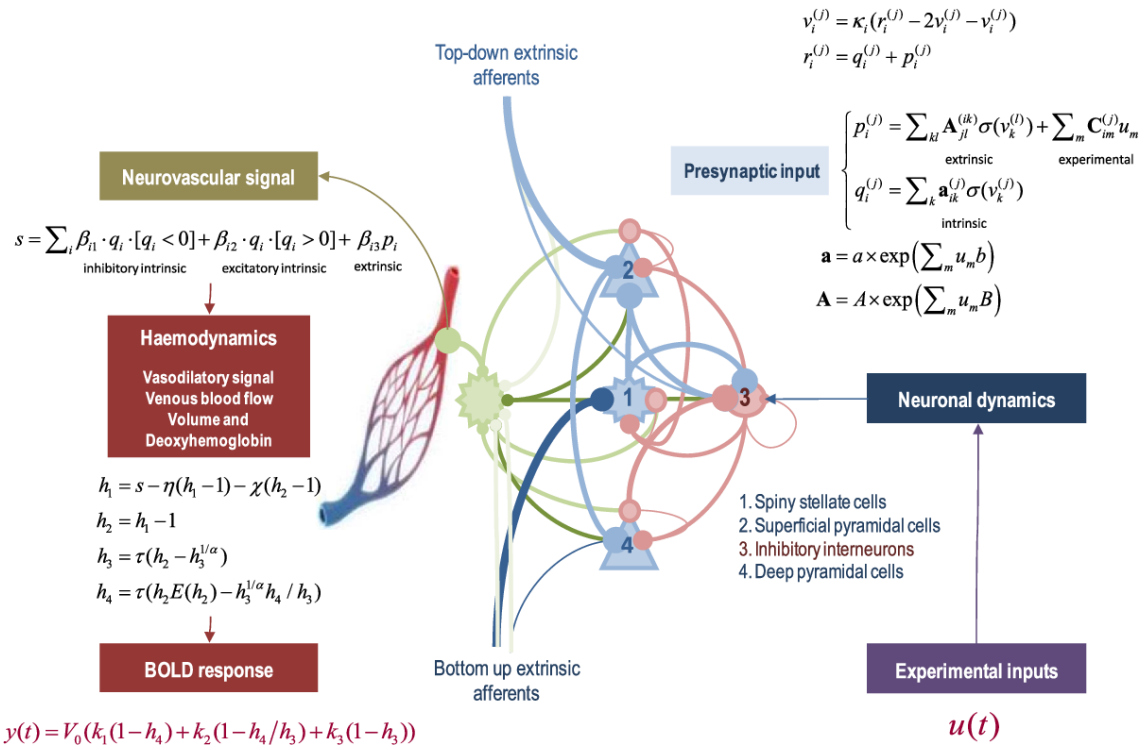

Fig.4. Schematic summarizing the generative model for each region or node. (Friston, K. J., 2017)

The signals arising from a neural network can be thought of a directed graph. Each node represented the functionally segregated source, while the edge describes the effective connectivity between pairs of nodes. In brief, experimental and extrinsic input at the specific node that responds to receive information, and then project to other nodes. The network is decided by between-node or extrinsic connectivity, and the distinction between forward and backward connections define the hierarchical relationships in the network, which corresponds the correlations among cortical and subcortical areas.

The DCMs describes the influences of experimental conditions or manipulations on the dynamics of neural states of the system. In fMRI, the changes of neuronal state that modulated the experimental condition drive the local changes in blood flow, which inflates blood volume and reduces deoxyhemoglobin content.

1.1.7 The present study

Despite the importance role, not only in daily life but also the clinical implications, many questions about the underlying neural mechanisms still remains unknown. For example, how does the brain dynamically adapt to the changing environment by flexibly adjust its control, and how does the brain be able to complete the balance between preparation and stop the response. In current thesis, the first study aims to examine these questions using functional magnetic resonance imaging (fMRI), and to further our knowledge about the cognitive control especially the inhibitory control of movement. I hypothesized that there are overlapping regions in the neural systems involved in proactive and reactive inhibitory processes. However, the effective connectivity between the relevant brain regions are modulated differently in those processes, which results in the different kinds of inhibitory control.

In the present study, I used a special neuroimaging contrast to isolate fMRI activity associated with proactive inhibition via the stop-signal paradigm, then identify

the brain areas involved in proactive and reactive inhibition. I then incorporated the identified regions of interest (ROIs) into dynamic causal models of proactive and reactive inhibition. Bayesian model selection (BMS) was applied to investigate the effective connections associated with each type of inhibition.

1.2 Materials and Methods

1.2.1 Participant

Twenty healthy right-handed adults (age, mean ± SD, 21.75 ± 2.57; range: 19–31 years; 11 males), excluding 10 participants with excessive head movement in the MRI scanner defined as translational or rotational displacement greater than 2.5 mm in any direction, performed a stop-signal task during fMRI scanning. All participants were recruited from the University of Tsukuba as paid volunteers, had normal or corrected-to-normal vision and provided written informed consent prior to the experiment. No participant was taking medicine during the experiment. The present study was approved by the Institutional Review Board (IRB) of the National Institute of Advanced Industrial Science and Technology (approval number: 2014-481) and all participants gave informed consent prior to participation.

1.2.2 Stop-signal task

In the present study, I divided the “go,” “stop,” and “switch” trials into several substages to isolate proactive and reactive inhibition. Unlike previous studies regarding proactive inhibition, I did not use additional cues to indicate “certain go” trials. All trials of the present study remained “uncertain” at the initial stage. During each trial, a fixation cross appeared on a black background for 500 ms, then the point of fixation

cross was replaced by the initial character ("X" or "O") for 1,500 ms. Participants were required to press "1" on the button-box if the stimulus was "X" and "2" if "O" appeared unless the background color change. If the background color changed to blue, participants need to switch their response to press "3." If the background color changed to red, participants are instructed to withhold their response regardless of the current initial character. The duration between the appearance of initial character and the change of background color is 500 ms. Thus, participants were required to withhold their planned response and wait for any possible upcoming cue to avoid an incorrect response when the initial character ("X" or "O") appeared. Participants must totally abort the responses that are already in progress if the background changed to red or switch their response to press "3" if the background changed to blue. The proactive component was thus present in all trials ("go," "stop," and "switch" trials), and the reactive component was present in successful "stop" and "switch" trials.

Each run consisted of 40 "go" trials, 10 "stop" trials, and 10 "switch" trials. An equal distribution of the characters "X" and "O" was ensured across trials, in random order. Each participant needs to complete three runs.

I applied paired *t*-test on mean RTs for "go" and "switch" trials to test if there were significant difference between them. Because the fixed stop-signal delay (SSD)

was used in the current procedure, I estimated SSRT with integration method by subtracting SSD from the finishing time that is determined by the distribution of no-signal go RTs.

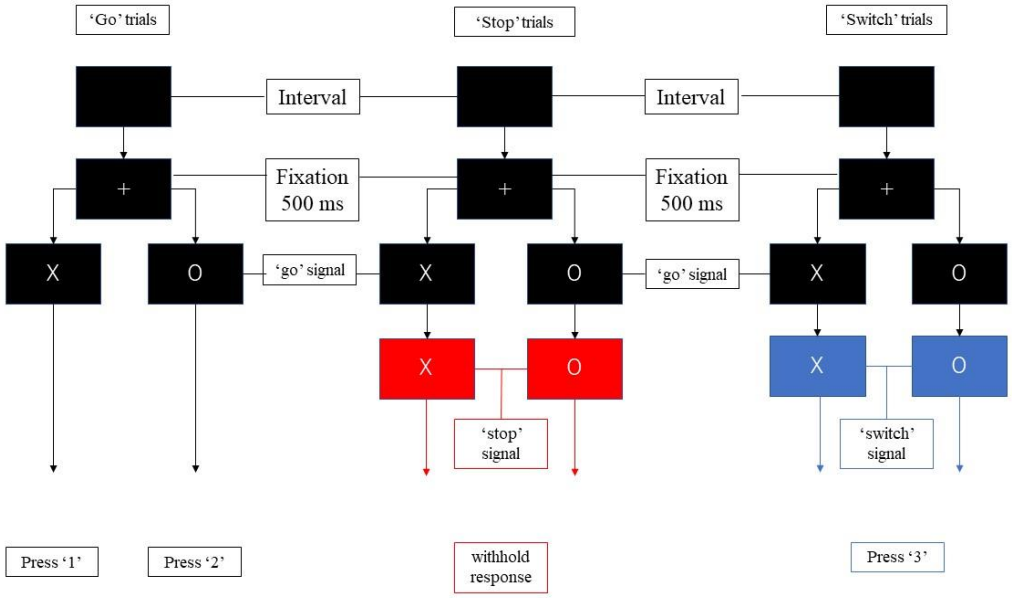

Fig.5. The components of the stop-signal task. Participants were required to press "1" or "2" as quickly as possible following the appearance of the stimulus unless the color of the background changed to red or blue. They were required to withhold response when the background turned red, and to press "3" when the background turned blue.

1.2.3 Procedure

All participants were informed about the MRI safety at the beginning of experiment. Each participant was provided with an information sheet that informed their participation rights before the experiment. After reading the information sheet and

signing the consent form, each participant was required to take the practice session in order to be familiar with the experimental procedure. The practice session consisted of three parts, each part includes two “go” trials, two “stop” trials and two “switch” trials. Feedback was provided on the computer monitor after the end of each trial by displaying the accuracy of each trial. The participant is required to take the practice session again if the accuracy was too low.

After the practice session, each participant was checked whether the metallics were carried and positioned inside the scanner. In order to minimize undesirable head motion, the participants were instructed to refrain from moving their head and limbs during the scanning. T1-weighted anatomical images were acquired before the participant was presented with a stop signal task. After the stop signal task, the participant was required to execute the DTI scanner. The participant could withdraw from the scanner and end the experiment at any time.

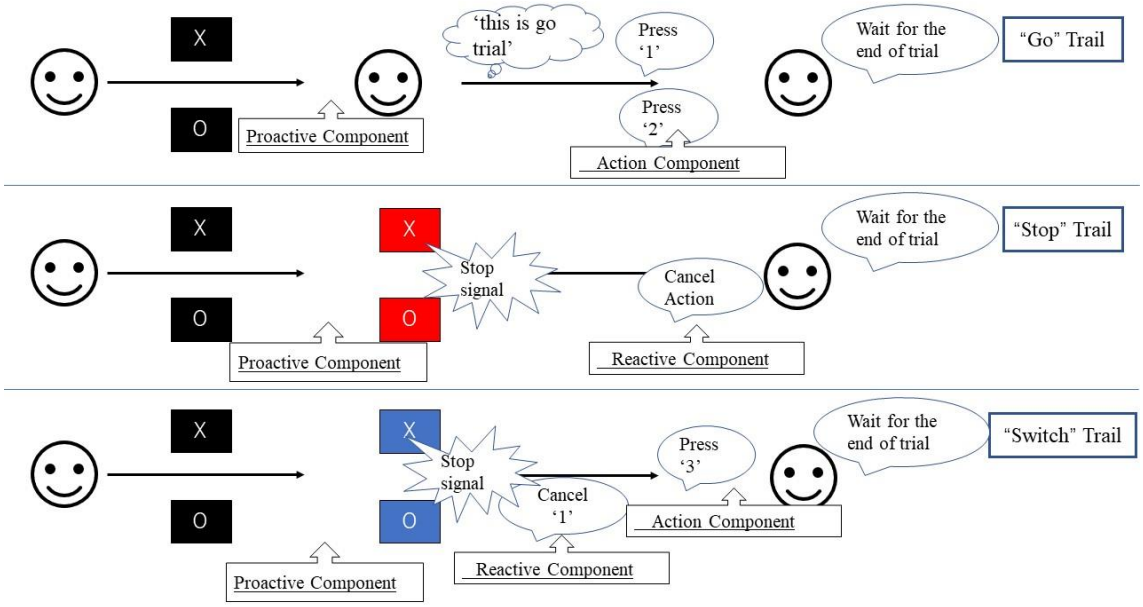

Fig. 6. Experimental paradigm used in this study.

1.2.4 fMRI Data Acquisition

All fMRI scans were obtained using a 3-Tesla scanner (Ingenia 3T, Philips, Netherlands) at the Department of Information Technology and Human Factors, AIST (Tsukuba, Japan). Each participant's head was fixed using foam padding to reduce head movement. Single-shot echo-planar imaging (EPI) sequences were used to acquire functional images. EPI parameters were as follows: repetition time (TR) = 2,000 ms; echo time (TE) = 35 ms; flip angle = 90°, 31 ascending slices, thickness = 3.7 mm.

1.3 Analyses

1.3.1 Data Processing

The SPM12 software toolbox and Matlab 2015b were used for the analysis of fMRI data and for the creation of the DCMs. All coordinates are reported in standard Montreal Neurological Institute (MNI) space and were labeled using the Anatomical Automatic Labeling (AAL) toolbox in SPM12 (Brett et al., 2002; Tzourio-Mazoyer et al., 2002). Successful “go” trials were regarded as those in which the participant selected the appropriate button following the waiting period. Successful “stop” and “switch” trials were regarded as those in which the participant withheld appropriate responses until the subsequent signals appeared.

I divided the trials into several components. All trials of the present study remained “uncertain” at the initial stage. When the initial character (“X” or “O”) appeared, participants were required to withhold their planned responses and wait for any possible upcoming cue to avoid an incorrect response. Thus, the proactive inhibitory component appeared at the beginning of all trials. The action component was involved when participants figured out the “go” trial and pressed the corresponding button. For both “stop” and “switch” trials, participants needed to cancel the planned

action that resulted in reactive inhibitory component. The difference is in “switch” trial, participants needed to press the alternative button, which led to subsequent action component. Based on the above reasons, the components in the “go” trials included proactive inhibitory component and an action component. The “stop” trials were subdivided into a proactive and a reactive component, and the “switch” trials consisted of a proactive, a reactive, and an action component.

Based on this approach, reactive inhibition was analyzed by comparing the successful “switch” trials to successful “go” trials. I did not apply the classical comparison that used for race model between successful “stop” trials (proactive inhibitory component + reactive inhibitory component) and successful “go” trials (proactive inhibitory component + action component) because the result cannot be explained by isolated reactive inhibitory component. Proactive inhibition was isolated by the conjunction of all successful trials (“go,” “stop,” “switch”). I used a general linear model for first-level event-related analysis in each participant. Events (successful “go,” successful “stop,” successful “switch”) were modeled after a duration of 0.5 s from trial onset. A second-level SPM analysis used contrasts from the first level with one-sample tests to investigate the group-level activation. A peak-level false discovery rate (FDR) at $p < 0.05$ was applied to correct for multiple comparisons.

1.3.2 Dynamic Causal Modeling for Comparing Proactive and Reactive Modulation

I used DCM12 (Friston et al., 2003) for the analysis of effective connectivity between the prior selected set of brain regions. fMRI-based DCM is a deterministic model of neural dynamics that describes how neural activity and interactions generate the hemodynamic BOLD response. The effective connectivity between brain regions or nodes was estimated by three matrices: the endogenous connectivity between nodes (A matrix), the modulation effects on the connection during the special experimental conditions (B matrix), and the driving inputs that influence the connectivity to other nodes (C matrix). If there were connections modulated by other regions (nonlinear connectivity effects), the parameters were modeled as an additional matrix (D matrix).

I defined MNI coordinates of the ROIs for DCM analysis that met all of the following criteria: (1) the coordinate of the spherical ROIs should show significant activations in both proactive and reactive contrasts with a cluster-based FDR at $p < 0.05$ in the second-level SPM analysis; and (2) the regions have been reported to be involved in behavioral control in previous research. I constructed 70 DCM models on four regions: the right IFG ($x = 48$, $y = 16$, $z = 30$), the left SMA ($x = -6$, $y = -10$, $z = 50$), the STN ($x = -10$, $y = -14$, $z = -6$), and the M1 ($x = -30$, $y = -12$, $z = 66$).

The set of 70 DCM models was divided into two groups: a linear and a nonlinear group. Each group was divided into several subgroups based on the location of the proactive modulatory input (IFG to SMA, SMA to IFG, IFG to STN, SMA to STN) and the connectivity between the IFG and the SMA (bidirectional, unidirectional, no connection; Figure 3). Average self-connections were applied to all nodes. The STN was connected with the IFG and the SMA directly or indirectly.

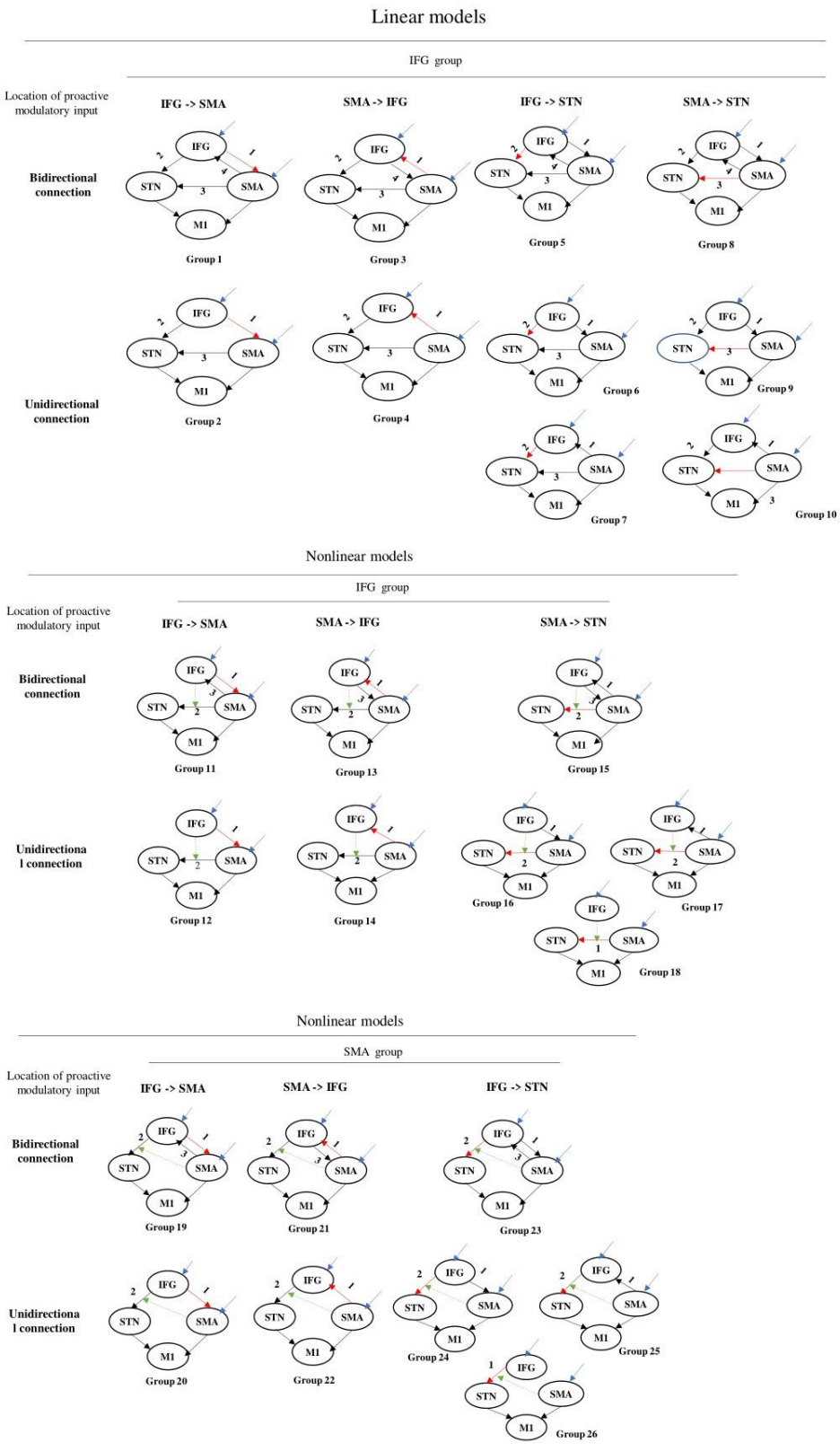
Linear models
IFG group
Location of proactive modulatory input
IFG -> SMA
SMA -> IFG
IFG -> STN
SMA -> STN
Bidirectional connection
Unidirectional connection
IFG
STN
SMA
M1
Group 1
Group 2
Group 3
Group 4
Group 5
Group 6
Group 7
Group 8
Group 9
Group 10
Nonlinear models
IFG group
Location of proactive modulatory input
IFG -> SMA
SMA -> IFG
SMA -> STN
Bidirectional connection
Unidirectional connection
Group 11
Group 12
Group 13
Group 14
Group 15
Group 16
Group 17
Group 18
Nonlinear models
SMA group
Location of proactive modulatory input
IFG -> SMA
SMA -> IFG
IFG -> STN
Bidirectional connection
Unidirectional connection
Group 19
Group 20
Group 21
Group 22
Group 23
Group 24
Group 25
Group 26

Fig. 7. Structure of the DCM families tested for proactive and reactive inhibition. Red arrows represent the locations associated with the proactive modulatory input. Dotted arrows represent the nonlinear modulation. The different numbers represent the different locations related to the reactive modulatory input. DCM, dynamic causal modeling; M1, primary motor cortex; IFG, inferior frontal gyrus; DLPFC, dorsolateral prefrontal cortex; STN, subthalamic nucleus; SMA, supplementary motor area.

The nodes, which receive driving input, are the regions in the model that first experience the neural changes caused by the manipulations of the experimental conditions. The modulatory inputs, which represent the specific experimental factor, realize the modulation by influencing the intrinsic connections in the network (Penny et al., 2004). Thus, the experimental conditions we chose as modulatory inputs should include the specific experimental factor and avoid the other factors that may drive the network activity in different modulatory effects. Both experimental conditions, that is, "stop" and "switch" trials, include the reactive inhibitory component, and for this reason, I selected all "go" trials (correct "go," incorrect "go") as proactive modulators to separate proactive from reactive modulation. I considered the frontal regions (IFG and SMA) as nodes receiving driving inputs across all models. The modulatory inputs include proactive modulatory inputs and reactive modulatory inputs. I applied the modulatory inputs in the fronto-STN connections (IFG to SMA, SMA to IFG, IFG to

STN, SMA to STN). All trials ("go," "stop," "switch") were chosen as driving inputs, which represent the extrinsic influences on the IFG-SMA-STN-M1 network. To separate proactive from reactive modulation, I selected all "go" trials (correct "go," incorrect "go") as proactive modulator. The reactive modulator was acquired by selecting "stop" and "switch" trials in which participants provided appropriate responses following the appearance of the signal.

I defined group peak coordinates from the second-level group analysis of proactive and reactive contrasts, combined with the AAL atlas implemented in the SPM toolbox. All trials were used for extracting the first eigenvariate of the BOLD time series for STN and M1, and the conjunction contrast of proactive and reactive modulators for IFG and SMA. All first eigenvariates were adjusted for the F-test of effects of interest. To extract the time series from the ROIs for each participant, I combined the local maximum close to the group peak and extracted the eigenvariate from a 5-mm sphere.

1.4 Results

1.4.1 Behavioral Data

There were significant differences in mean RTs between “go” trials (mean ± SD, 963 ± 74 ms, range: 836–1092 ms) and “switch” trials (mean ± SD, 1,120 ± 87 ms, range: 948–1,350 ms; $p < 0.0001$). For “go,” “stop,” and “switch” trials, mean accuracy was 0.890 (SD: 0.117) and 0.853 (SD: 0.165), respectively. The mean SSRT was 454 ms (range: 304–737 ms, SD: 96 ms).

1.4.2 Group-Level Activations

Activity associated with proactive inhibition obtained by the conjunction of all successful “go,” “stop” and “switch” trials, was significant in the visual cortex, dorsolateral prefrontal cortex (DLPFC), caudate, SMA, IFG, STN and M1 of both hemispheres. As for the reactive inhibition, I found activation in the right IFG, the left SMA, left M1, as well as bilateral activation of STN (Figure 8). Because the volume of STN is about 240 mm3 in humans that means the activation of STN is only eight voxels (Hardman et al., 2002; Hamani et al., 2004), I chose the coordinate of the STN described in Forstmann et al. (2012) as a reference to confirm the STN activated significantly.

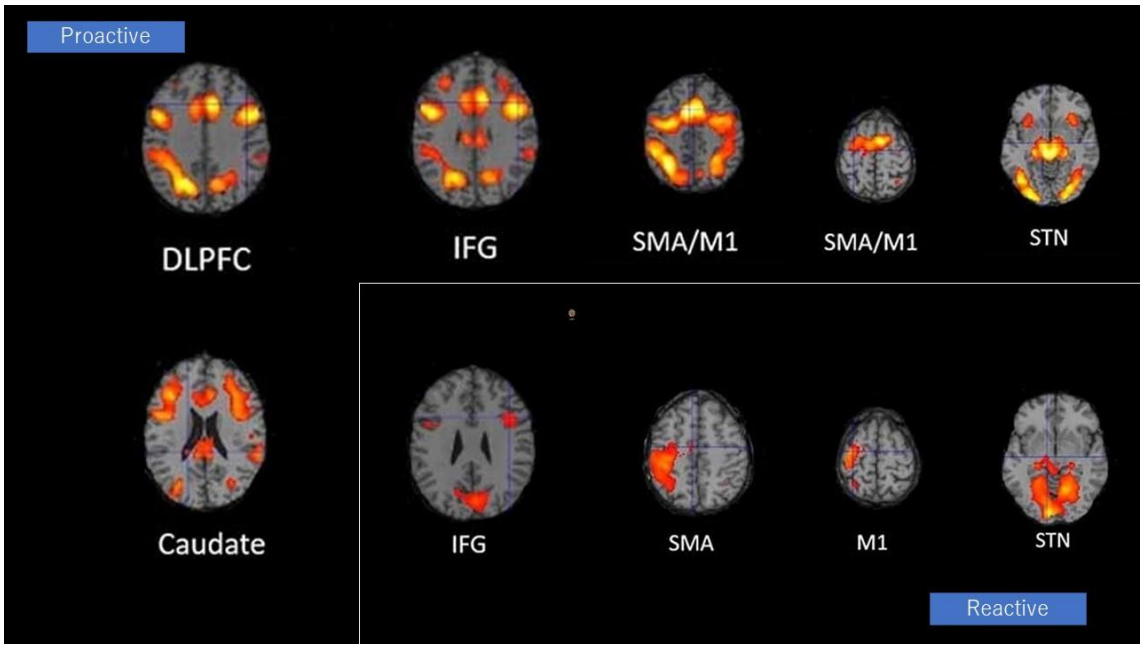

Fig. 8. Activated brain regions associated with (1) proactive inhibition and (2) reactive inhibition during the stop-signal fMRI experiment. Group-level statistical maps were calculated (1) as conjunction of all successful "go", "stop" and "switch" trials for proactive inhibition and (2) as a contrast between successful "switch" trials and successful "go" trials for reactive inhibition. The results were thresholded at peak-level false discovery rate (FDR)-corrected significance of $p < 0.05$.

1.4.3 DCM Network Analysis for Comparing Proactive and Reactive Modulation

I investigated 70 DCMs representing the alternative hypotheses of modulatory effects from proactive and reactive inhibition. BMS with fixed-effect analysis (FFX) provided strong evidence for one model being optimal, above all other models.

Two parameters were measured in the BMS to compare the optimal architecture of the models: relative log-evidence and posterior probability. The former corresponds

to the balance between accuracy and complexity of the model, while the latter represents the probability that the specific model provides the best explanation for all participants.

DCM estimates the observed BOLD responses and models the effects of neuro-vascular processes and spectral noise at different levels. The parameters represent the rate of change in activity in one region that influences the activity in another region, and the effective connectivity was thus expressed in Hz.

The average connectivity between two regions represents how rapidly activity (per second) in one region influences the activity in another region (Friston et al., 2003; Penny et al., 2004; Almgren et al., 2018). A positive value represents an excitatory influence from the source region on another region, while a negative value represents an inhibitory influence. Likewise, modulatory effects on a region or connection indicate an increase or decrease in average activity or connectivity.

In this optimal nonlinear model, the right IFG modulates the connection between the left SMA and the left STN, and the connection from the IFG to the SMA is modulated by both proactive (modulation effect = 0.8622 HZ) and reactive modulatory inputs (modulation effect = 0.8404 HZ). The results indicate that when people “prepare to cancel” and then “cancel” a planned response successfully, both proactive and

reactive modulation influence on the effective connection from the IFG to the SMA. The IFG inhibits the activity in the SMA, and the decreased activity in the SMA influences the subsequent areas via a causal relationship and then increases the excitatory influence of the STN on the M1.

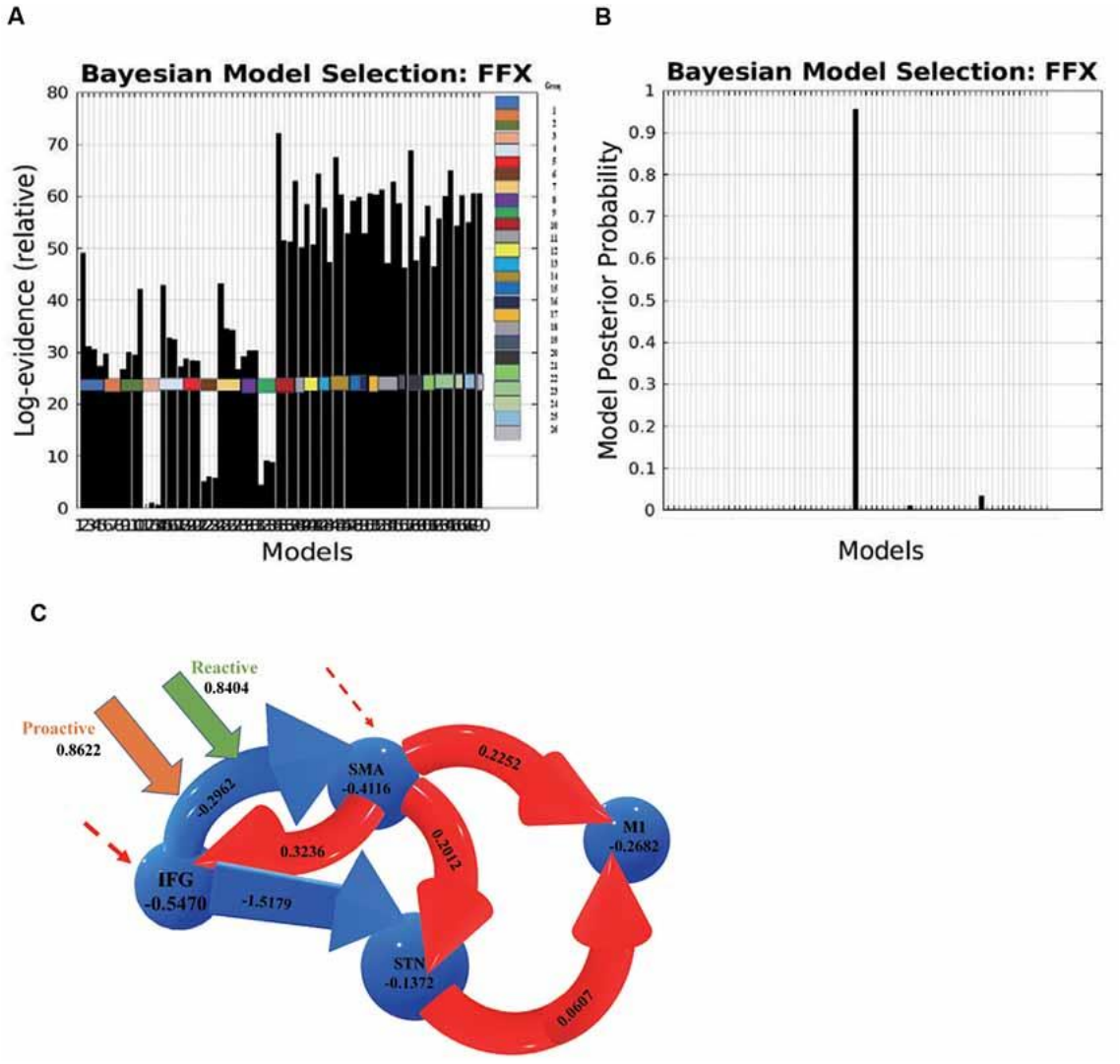

Fig. 9. (A) Log evidence and (B) model posterior probability to compare DCM model families, and (C) the most possible model selected based on Bayesian model selection (BMS) denoting connectivity coefficients for the comparison between proactive and reactive modulatory inputs. The connections in red

represent increased excitatory connectivity, while blue connections represent decreased inhibitory connectivity. The dotted lines represent the driving inputs.

1.4.4 DCM Network Analysis for Proactive Inhibition

To further investigate the possible brain circuits involved in the implementation of behavioral control including proactive and reactive inhibitory processes, I added extra regions to the DCM models for proactive inhibition. The regions of interests were selected based on the same criteria as the previous DCM models, i.e., (1) these regions should show significant activation in proactive contrasts with a cluster-based FDR at $p < 0.05$ in the second-level SPM analysis; and (2) the regions have been reported to be involved in behavioral control in previous research. I constructed 13 DCM models including four ROIs: the right IFG, the DLPFC ($x = 44$, $y = 20$, $z = 36$), the left SMA, and the caudate ($x = -16$, $y = -30$, $z = 24$). As previous results showed that the modulatory effects were related to the connection from the IFG to the SMA, this modulatory effect should be a direct or indirect effect from other effective connections that end in the IFG.

I limited the model for proactive inhibition to the four regions based on the following reasons: (1) the previous studies suggested the top-down control for proactive inhibitory control (Jaffard et al., 2007, 2008; Criaud et al., 2012). Based on the result

from the DCM network analysis for comparing proactive and reactive modulation, it revealed that the modulatory effects happened on the effective connectivity from IFG to SMA. Thus, it is reasonable to believe that the proactive modulation would not firstly act on the downstream connections that causally follows the effective connection from IFG to SMA; and (2) the increasing number of nodes in DCM will lead to over much numbers of free parameters that require exponentially increasing computational time. Furthermore, the conditional dependencies among these parameters will also enhance that influence the reliability of explanation for DCM model (Daunizeau et al., 2011). Based on these reasons, I think the model with four regions DLPFC-caudate-IFG-SMA is sufficient to investigate the proactive modulation.

Since converging evidence indicates that the prefrontal areas project to the STN, in the DCM analysis of proactive inhibition, the DLPFC-IFG-SMA-caudate is the minimum and effective set required to test hypotheses. I have found reactive modulatory effects on effective connection from IFG to SMA in the previous step, so there are two possibilities for the "real" neural underpinning of reactive modulation: (1) the IFG-SMA is the real effective connectivity that is modulated by reactive inhibition; and (2) the real effective connectivity is the other connectivity in prefrontal-STN network. The modulatory effect was transferred to the effective connectivity IFG to

SMA and observed in the IFG-SMA-STN-M1 DCM model. Based on the result from whole brain contrast related to reactive inhibition, there are no other activations in frontal areas involved in inhibitory control and prefrontal-STN connections, which means no other effective connectivity responds to reactive inhibition, so the IFG-SMA is the real effective connectivity that modulated by reactive inhibition.

The set of 13 DCM models was divided into three groups based on whether the DLPFC receives driving inputs (driving inputs were applied to DLPFC + SMA, IFG + SMA, and DLPFC + IFG + SMA). The location of proactive modulatory inputs varied in the bidirectional connections in the DLPFC-IFG-SMA-caudate network, and locations were chosen based on the requirement that the indirect modulatory effects from other effective connections should end in the IFG. Average self-connections were applied to all nodes. The interconnectivities between nodes are bidirectional (Figure 10). I considered the frontal regions (DLPFC and SMA, IFG and SMA, DLPFC/IFG/SMA) as nodes receiving driving inputs across all models. The modulatory inputs are only proactive inputs. I applied modulatory inputs to the effective connections in the DLPFC-caudate-IFG-SMA network (IFG-DLPFC, DLPFC-IFG, IFG-SMA, DLPFC-caudate, caudate-IFG).

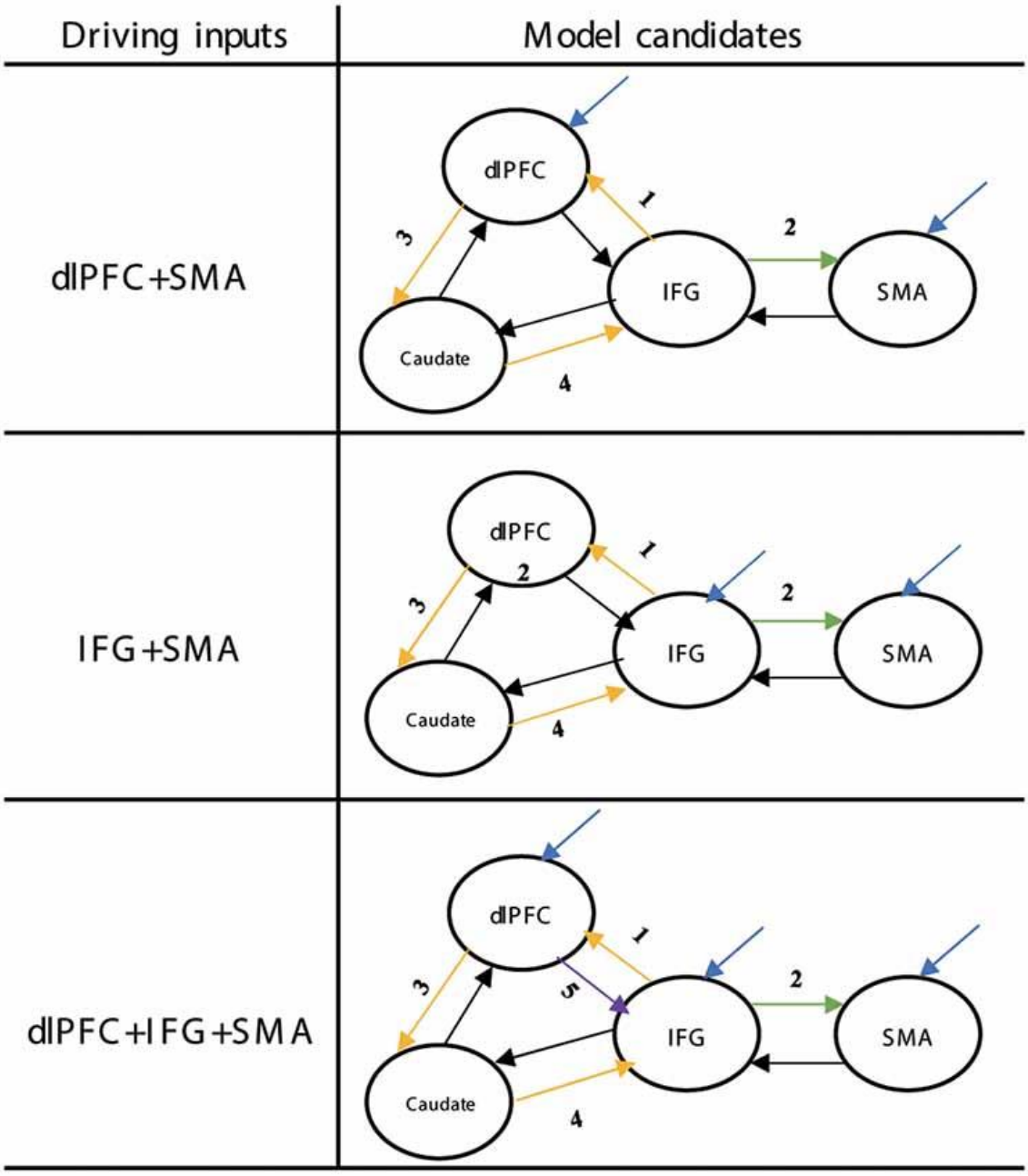

Fig. 10. Structure of the DCM families tested for proactive inhibition. The yellow arrows show the direction of loops that represent indirect modulation from other effective connections that end in the IFG. The different numbers represent the different locations related to the proactive modulatory input. DCM, dynamic causal modeling; M1, primary motor cortex; IFG, inferior frontal gyrus; DLPFC, dorsolateral prefrontal cortex; STN, subthalamic nucleus; SMA, supplementary motor area.

I extracted the first eigenvariate of the BOLD time series from two regions of interests, the DLPFC and the caudate. All-time series were adjusted for the F-test of effects of interest. To extract the time series from the ROIs for each participant, I combined the local maximum close to the group peak and extracted the eigenvariate from a 5-mm sphere.

The results of BMS (FFX) indicated that there was one model that was superior to all other models (Figure 7). In this model, the connection from the caudate to the IFG was associated with the proactive modulation (modulation effect = 0.7851). The results indicate that when people prepare for a possible upcoming stop-signal, the caudate increases its excitatory influence on the IFG, which leads to an inhibitory influence of the IFG on the SMA.

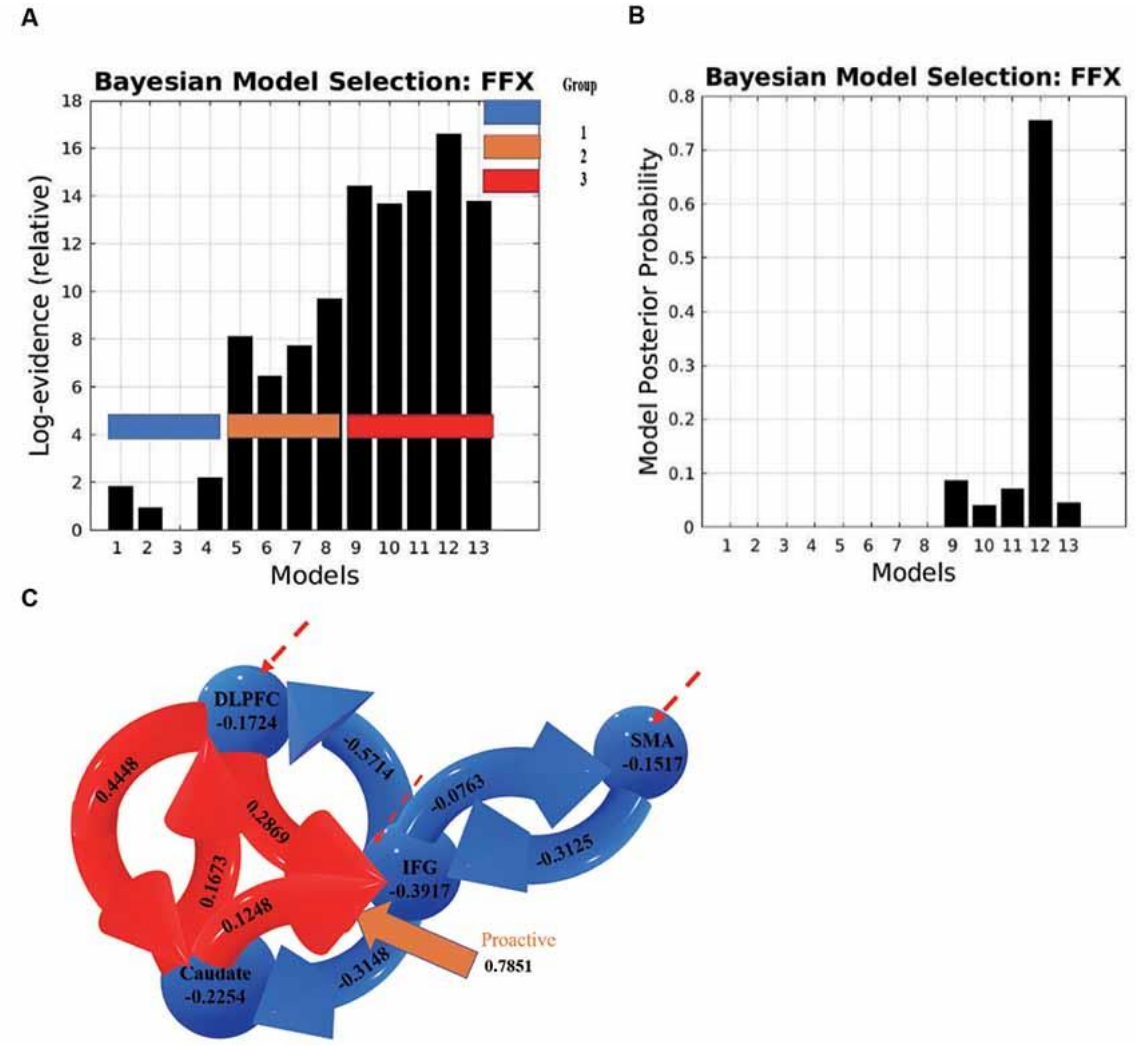

Fig. 11. (A) Log evidence and (B) model posterior probability to compare DCM model families, and (C) the most possible model selected based on BMS denoting connectivity coefficients for the DCMs with proactive modulatory inputs. The connections in red represent increased excitatory connectivity, and blue connections represent decreased inhibitory connectivity. Red dotted lines represent the driving inputs.

1.5. Discussion

In the present study, I used fMRI data acquired during a stop-signal paradigm task to identify the cortical and subcortical areas involved in proactive and reactive inhibitory processes. To evaluate the modulatory effects of proactive and reactive inhibition on the effective connections between these areas, I first conducted a DCM analysis where 70 DCM models were compared. The results indicate that the increasing activity in effective connectivity from the left SMA to the left STN was modulated by the right IFG, and the decreasing activity in effective connectivity from the right IFG to the left SMA was modulated by both proactive and reactive modulatory effects. I further investigated an alternative hypothesis with 13 additional DCM models in which the causal connection from/to the right DLPFC and the left caudate were considered for proactive inhibition. The results of the additional DCM model comparison show that the increased activity of the effective connection from the left caudate to the right IFG was modulated by proactive modulatory control, which resulted in the inhibitory effects in the connections from the right IFG to the left SMA in the comparison between proactive and reactive inhibitory control.

The fronto-basal ganglia pathways have been proposed to support motor control via hyper-direct and indirect pathways. Previous studies suggested that the right IFG

and left SMA are critical regions in inhibitory control (Aron et al., 2004; Chambers et al., 2006; Aron et al., 2014). However, it is still difficult to assign a very specific role to most of these regions during the execution of complex cognitive functions (Mirabella, 2014; Hampshire, 2015). For example, some studies revealed that the right IFG acts as a monitor of unexpected stimuli, and others show that it is involved in the suppression of memories.

A significant overlap was reported in the brain systems underlying proactive and reactive inhibition via modified stop signal task or extra information about the probability of the occurrence of stop signals, and showed that the right IFG, the pre-SMA/SMA, and part of the basal ganglia circuit (striatum) are involved in both proactive and reactive inhibition (Chikazoe et al., 2009a; Swann et al., 2012; Aron et al., 2014). Furthermore, the recent research reveals that the neural network involved in goal-directed cognitive control is very extensive. The multi-step decision process model proposed that many areas such as the DLPFC, PMd, and M1 are also involved in goal-directed behavior (Kenner et al., 2010; Mirabella, 2014). However, previous studies were unable to determine the interactions that exist between these regions or to describe how the brain can “identify” the different kinds of inhibitory control.

I used DCMs to demonstrate which connections in the common network contribute to proactive and reactive inhibitory control. The DCMs also provided us with information regarding the directions and excitatory or inhibitory modulatory effects of these connections. The results reveal that the effective connection from the IFG to the SMA is associated with both proactive and reactive modulatory effects, which is in line with previous neurophysiology and neuroimaging evidence showing that the IFG is connected with the SMA. The results further show that in the most likely model, both proactive and reactive inhibition decreased the excitatory influence from the IFG to the SMA and inhibited the activity of M1.

The results of further investigation of proactive inhibition show that the neural underpinning of proactive modulation is the effective connection from the right DLPFC via the left caudate to the right IFG, while the subsequent effect of transmission is reflected in the effective connection from the IFG to the SMA in a common network. The brain thus uses the DLPFC-caudate-IFG-SMA-STN-M1 pathway to implement proactive modulation. These results support the prior hypothesis that basal ganglia circuits are involved in proactive and reactive inhibition, which suggested that a hyperdirect pathway that allows for faster behavioral control than the direct and indirect pathways, by bypassing the striatum, is involved in reactive inhibition. The indirect

pathway is functionally similar to the hyperdirect pathway but transfers the modulatory effects through the striatum.

The present study also provides new evidence for the functions of the right IFG. Although previous studies have extensively investigated the role of the right IFG in response inhibition, findings remain controversial. It remains, for example, unclear whether the right IFG is associated with modulatory inhibition or with the more general detection of salient or task-relevant cues. Furthermore, the right IFG is considered to expedite inhibition processes via the pathway from the pre-SMA/SMA to subcortical regions, based on findings from neuroimaging and transcranial magnetic stimulation studies (Aron et al., 2003; Chambers et al., 2006). However, electrophysiological studies have indicated that activity in the pre-SMA/SMA can precede activity in the IFG during response inhibition (Swann et al., 2012). The results indicate that the right IFG acts as a driving input during reactive inhibition, supporting the notion that this region plays a key role in detecting task-relevant cues. These results, therefore, suggest that the IFG is related to attentional switching. These results are consistent with previous findings showing that right-IFG activity was higher when infrequent stimuli were detected, indicating that this region does not belong to a unique network involved in inhibitory control (Hampshire et al., 2010; Erika-Florence et al., 2014).

The study furthermore provides evidence for the functions of the right DLPFC. Comparative studies involving both humans and non-human primates have concluded that the PFC is a crucial neural substrate of cognitive control (Servan-Schreiber et al., 1996; Assad et al., 1998; Cohen et al., 1999; Jahfari et al., 2012; Smittenaar et al., 2013). Recent studies have also revealed that the DLPFC plays a central role in the maintenance of goals and rules for action (Watanabe, 1990, 1992; Asaad et al., 2000). Additional studies have demonstrated that the DLPFC monitors environmental cues to develop appropriate response strategies (Ragozzino, 2007; Hikosaka and Isoda, 2010). These findings are consistent with the result that the DLPFC acts as a driving input during proactive inhibition.

Previous tract-tracing studies in monkeys and diffusion tensor imaging studies in humans have indicated that the DLPFC is connected with the caudate (Parent, 1990; Parent and Hazrati, 1995; Lehéricy et al., 2004), and that the DLPFC-caudate circuit is involved in selective inhibition via the indirect pathway (Mink, 1996; Jahfari et al., 2011). Previous animal, clinical, and neuroimaging studies have provided extensive evidence that the caudate was involved in the selection of appropriate response based on the assessment of the outcomes, and the studies of patients with impairments in the caudate nucleus also showed the deficit in goal-directed tasks (Hazrati and Parent, 1992;

Cai et al., 2011; Bryden et al., 2012; Majid et al., 2013). The results indicate that the left caudate is related to modulatory input, consistent with the findings of previous studies reporting that the caudate nucleus contributes to behavior through the selection of appropriate sub-goals.

In the current study, I used fMRI to investigate inhibitory behavior. The limited temporal resolution of fMRI may result in limited scope in the DCM analysis. Therefore, multiple methods such as electroencephalography (EEG) or ECoG, which have better temporal resolution, need to be considered in future research. Further, I had to exclude participants with excessive head movement, and the reduced number of effective participants might have caused us to miss some regions with significant activations.

1.6 Conclusion

I show that the effective connection from the IFG to the SMA is associated with reactive inhibition, while the effective connection from the caudate to the IFG is associated with proactive inhibition. The indirect DLPFC-caudate-IFG-SMA-STN-M1 pathway is involved in the implementation of proactive modulation, while the hyperdirect pathway that bypasses the striatum contributes to reactive inhibition. The function of the IFG is more related to attention control, and the caudate more likely acts as a “gate” between proactive and reactive inhibition.

Study 2: Correlations between white matter microstructure infers the effective connectivity in response inhibition

Introduction

The first study investigated the brain areas involved in response inhibition and the causal architecture between the fronto-basal ganglia circuit. I applied the dynamic causal models to fMRI data and found the "longer" DLPFC-caudate-IFG-SMA-STN-M1 pathway is associated with the implement of proactive inhibition, while the "shorter" IFG-SMA-STN-M1 pathway that bypasses the striatum is modulated by the reactive inhibitory modulation (Zhang and Iwaki, 2019).

The result from DCM revealed the crucial roles of frontal areas and basal ganglia in response inhibition, so it is naturally to discuss whether there exists a correspondence relationship between the functional and structural architecture. Diffusion Tensor Imaging (DTI) allows the application of the noninvasive measurement of structural connectivity in vivo (Basser and Pierpaoli, 1996; Pierpaoli et al., 1996). Thus, in the second study, I investigated the anatomical connections existing in the fronto-basal ganglia circuits via DTI and probabilistic fiber tractography, and whether

the corresponding relationship exists between fMRI signals as a functional manifestation in response inhibition and the structure of the brain.

2.1 Theoretical background

An open question in the brain research is the correspondence between functional and structural pathways. Given that the neural underpinning for response inhibition has been studied by functional MRI in the past decade, and the first study also identified the neural pathways between frontal cortex and basal ganglia engaged in successful response inhibition (Alexander et al., 1986; Albin et al., 1989; DeLong, 1990; Nambu et al., 2000, 2002; Aron et al., 2007a,b; Baker et al., 2010; Dunovan et al., 2015; Mallet et al., 2016; Zhang and Iwaki, 2019), it is naturally to explore the linkage between the anatomical connectivity and the functional interactions (Honey et al., 2010; Werring et al., 1999). Diffusion Tensor Imaging (DTI) is a non-invasive technique that provides the information of white matter structure by analyzing the diffusion of water affected by the local brain tissues (Basser and Pierpaoli, 1996; Pierpaoli et al., 1996). The DTI parameters measured from regions of interest as well as tracts is sensitive to the degree of anisotropic water diffusion, which reflects the cellular structures in the white matter.

2.1.1 Diffusion Tensor Imaging (DTI)

DTI is a non-invasive technique for monitoring the neural architecture by measuring the degree of water molecules in the tissue. The theoretical foundation is based on the physical phenomena named random translational motion or brownian motion. The water molecules randomly colliding with each other in the brownian motion can be statistically described by a diffusion coefficient. The diffusion coefficient depends only on the molecular weight, the temperature and the certain conditions. Thus, the measurement of diffusion-driven displacement provides a direct method to investigate the micro-structure of brain tissue.

The diffusion propagation of water molecules has certain preferential directions in the brain parenchyma structures because of the boundaries on a microscopic scale. Thus, the molecular displacements are greater than other in some structures, which means the diffusion is more anisotropic. Conversely, some structures allow the water molecules move more freely with less constraint. In this situation, the diffusion is more isotropic. The difference in the molecular displacements is critical for the reconstruction of anatomical structure in the brain.

The typical diffusion times used for clinical DWI are 10 –50 ms, corresponding to average molecular displacements on the order of 10 um. This microscopic spatial scale is in the same range as that of cellular dimensions. This sensitivity to cellular

processes has been exploited clinically for improving the detection of acute cerebral ischemia (Thomsen et al., 1987; Moseley et al., 1990; Chien et al., 1992; Warach et al., 1992; Marks et al., 1996; Gonzalez et al., 1999), distinguishing vasogenic from cytotoxic edema (Ebisu et al., 1993; Schaefer et al., 1997; Schwartz et al., 1998; Ay et al., 1998; Mukherjee et al., 2001; Provenzale et al., 2001), identifying foci of axonal shearing injury after acute head trauma (Arfanakis et al., 2002; Hergan et al., 2002; Huisman et al., 2003), characterizing cellularity in brain tumors (Tien et al., 1994; Brunberg et al., 1995; Krabbe et al., 1997; Gauvain et al., 2001), discriminating between metastases and gliomas (Krabbe et al., 1997; Lu et al., 2003), and between tumor recurrence and postsurgical injury, differentiating pyogenic abscesses from tumors (Smith et al., 2005), and for the noninvasive mapping of white matter connectivity by using the diffusion tensor model (Ebisu et al., 1996; Kim et al., 1998; Leuthardt et al., 2002), among the diffusion tensor model.

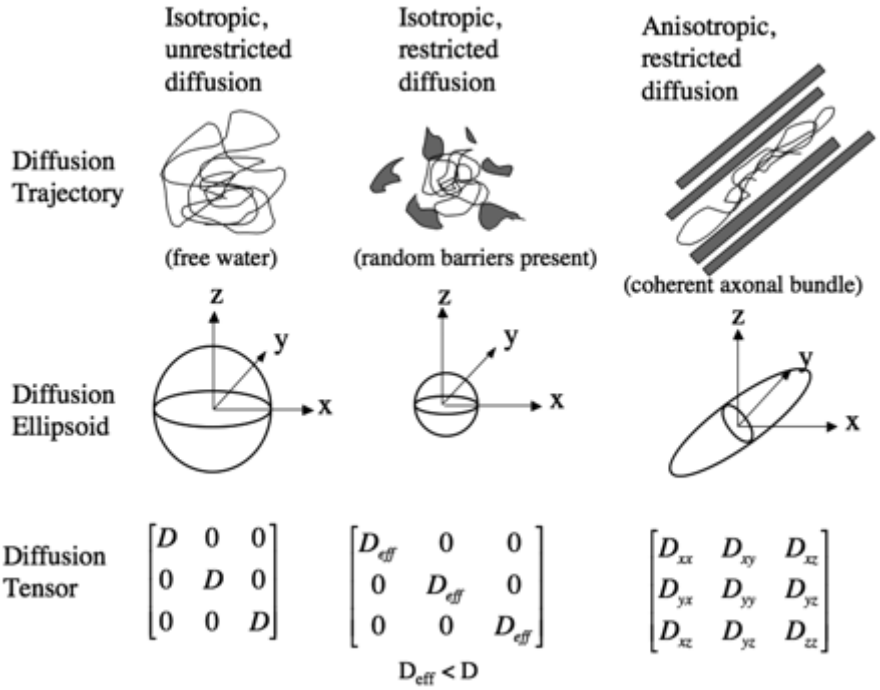

Fig.12. The diffusion ellipsoids and tensors for isotropic unrestricted diffusion, isotropic restricted diffusion, and anisotropic restricted diffusion. (Mukherjee, P. et al., 2008)

2.1.2 Fiber Tracking

DTI is currently the only non-invasive method to track the white matter fibers through the human brain, and tractography method quantifying the structural brain connectivity based on the assumption that the main diffusivity direction is aligned with the direction of the axonal fiber dominant within the voxel (Pajevic and Pierpaoli, 1999). The axonal fiber tracks are modeled by tracing the most favorable pathway between two voxels that calculated by fiber reconstruction algorithms.

The exact pathway of the axonal fibers is of less interest in most of cognitive studies than the degree of connectivity. This is the reason why the use of probabilistic

methods (Behrens et al., 2003) to determine the degree of connectivity is preferred, instead of line streaming approaches that are focused on the anatomical pathways of the fibers.

Fiber tract reconstruction requires first the selection of seed point, and the tracing is executed by spatially interpolating direction of maximum diffusion neighboring voxels (Kubicki et al., 2002). In this way, the use of the foci of functional activity as initial and ending tracking points, allows the connection between regions. This appears to be a very promising approach to integrating structural and functional information, which might be used to model the underlying neural network in a specific task.

2.1.3 Parameters of DTI measure

The parameters of DTI are sensitive to the degree of anisotropic water diffusion, which reflects the cellular structures. The measure of DTI parameters from regions of interest as well as tracts have been revealed the correlation with behavioral performance (Klingberg et al., 2000; Niogi et al., 2008b). The hypothesis is that the tissue microstructure such as axon diameter or myelination affect the nerve conduction velocity (Fields, 2008; Seidl, 2014) and then affect reaction time (Chevalier et al., 2015; Copra et al., 2018).

The DTI produces several metrics that summarize the properties of white matter microstructure (Basser & Pierpaoli, 1996; Pierpaoli, Jezzard, Basser, Barnett, & Di Chiro, 1996). Fractional Anisotropy (FA) is a metric derived from DTI that captures the degree to which water diffusion is restricted in a given region. Restricted water flow can arise from a multitude of factors such as more tightly packed axons or a higher degree of myelination, which may indicate a more efficient tract structure. FA is particularly sensitive to the orientation of white matter as well as its integrity.

2.1.4 Previous study about white matter microstructure and response inhibition

Previous studies have investigated the influence of structural connections in fronto-basal ganglia tracts in response inhibition. The analysis of probabilistic tractography between basal ganglia and the IFG, preSMA/SMA revealed the significant correlations between stop signal reaction time (SSRT) and DTI parameters in the cognitive control task (King et al., 2012; Lison et al., 2006; Casey et al., 2007; Rae et al., 2015). One such study examined go/no-go performance in parent-child dyads with Attention Deficit Hyperactivity Disorder (ADHD) and found that there was a positive correlation between FA in prefrontal regions and d-prime in both parents and children (Casey et al., 2007). These studies linked the frontostriatal microstructure with the functional activity and SSRT performance.

These studies have generally focused on the white matter tracts that connecting IFG, SMA and STN, and correlation with the performance of cognitive task. However, it remains unclear the correspondence between structural and functional connections as well as the possible neural dynamics in response inhibition, especially the separate neural activities underlying the proactive and reactive inhibition. So, the investigation of the correspondence between white matter structure and the dynamical connectivity in response inhibition will offer an opportunity to understand how the functional and dynamic connections are generated and mediated by direct or indirect anatomical structure.

2.1.5 The limitation of previous study

These studies have generally focused on the white matter tracts that connecting IFG, SMA and STN, and correlation with the performance of cognitive task. However, it remains unclear the correspondence between structural and functional connections as well as the possible neural dynamics in response inhibition, especially the separate neural activities underlying the proactive and reactive inhibition. So, the investigation of the correspondence between white matter structure and the dynamical connectivity in response inhibition will offer an opportunity to understand how the functional and

dynamic connections are generated and mediated by direct or indirect anatomical structure.

2.1.6. The current study

In the present study, I chose the regions for tract of interests based on results from the previous study where I used fMRI effective connectivity measures to demonstrate the involvement of IFG, SMA, DLPFC, caudate, STN and M1 in the hyperdirect and indirect neural pathways responding to reactive and proactive inhibitory control. Then I extracted the FA from the tract-of-interest and applied the hierarchical clustering to the white matter tracts. Furthermore, I examined the inter-tract correlations of FA with spearman's rank correlation coefficient. These results were combined with effective connectivity in response inhibition to investigate the correspondence between the structural structure and functional/effective network.

2.2 Materials and Methods

2.2.1 Stop-signal task and participants

Eleven healthy adults (age, mean±SD, 21.75±2.57; range: 19-31 years, males) performed a stop-signal task during fMRI scanning. Participants were recruited from University of Tsukuba as paid volunteers. The present study was approved by the institutional review board of the National Institute of Advanced Industrial Science and Technology (approval number: 2014-481). All participants were right-handed with normal or corrected-to-normal vision. Prior to the experiment, all subjects provided written informed consent.

Each participant needs to complete three runs for the stop-signal task paradigm, and each run consists of 40 go-trials, 10 stop-trials and 10 switch-trials. During each trial, a fixation cross appeared on the black background for 500 ms, then the fixation cross was replaced by the character “X” or “O” for 1500 ms. Participants should press “1” on the button-box if the character was “X” and “2” if it was “O”, unless the background color changed after a while. Participants had to switch their response to press “3” if the background color changed to blue, and totally abort their planned response if the background color changed to red. An equal distribution of characters “X” or “O” was applied to all trials in a random order (Zhang, F., and Iwaki, S., 2019).

2.2.2 DTI acquisition

Imaging data were acquired on a 3-Tesla scanner (Ingenia 3T, Philips, Netherland). The diffusion images were acquired using a single shot echo-planar imaging sequence (TR= 18.486 ms, TE= 60 ms, FA = 90 deg, 32 gradient directions. Matrix size: 224 x 224 x 140 mm (112 x 112 matrix), 2 mm slice thickness, 70 slices, b-factor = 1,000).

2.3 Data Analysis

2.3.1 DTI Data Pre-processing

DTI data were acquired from the same participants who participated the stop-signal task in the fMRI scanning during the same scan. Pre-processing of the DTI data were performed in the FSL 5.0 software (FMRIB's Software Libary, www.fmrib.ox.ac.uk/fsl) and matlab 2015. The B0 volume was firstly extracted and masked by using "fslroi" and "bet". Then the diffusion images were corrected by "eddy_correct" and diffusion tensors were fitted with "dtifit". For tractography, I used "bedpostx" to calculate the voxel-wise diffusion distribution at each voxel.

2.3.2 Probabilistic tractography between frontal cortex and basal ganglia

The group-level activations were found in the right IFG, the left SMA as well as bilateral STN in reactive inhibition, and the brain regions with significant activations were identified in DLPFC, caudate, IFG, SMA and STN in both hemisphere in the previous study. Considered the critical role of right IFG in response inhibition, I constructed the masks and analyzed the inter-tract interests only in the right hemisphere. I created masks of the right DLPFC, caudate, IFG, SMA and STN in MNI standard space, then these prior masks were transformed to each subject's native T1 space using "flirt".

I used FSL “probtrackx” to create the tracts of interest between: 1) the right DLPFC and right caudate, and 2(the right caudate and right IFG, and 3) the right IFG and right SMA, and 4) the right SMA and right STN, and 5) the right caudate and right STN, and 6) the right IFG and right STN. I thresholded 50% probability for each tract, which means only voxels showing at least 2500/5000 streamlines were retained in the result pathway. Then these thresholded tracts were transformed to each subject’s diffusion space by using “flirt” linear registration. The output masks were binarized by “fslmaths”. Each subject’s FA map was masked by the tracts and the average time-series was extracted using “fslmeants”. The average value of FA was acquired by “fslstats”.

2.3.3 Hierarchical clustering and correlation analysis

I used hierarchical clustering to investigate whether there are specific clustering patterns in white matter tracts between fronto-basal ganglia circuit. Hierarchical clustering model employed the functions in Matlab 2015. The dissimilarity between each pair of white matter tract in FA was calculated by “pdist” function, and the “linkage” function was used to pair the white matter tracts with close proximity. Then the formed clusters were grouped into larger cluster until a hierarchical tree was formed.

After the determination of clusters in white matter tracts, I used Spearman's rank correlation coefficient to measure all correlations between tract-of-interests. The result from hierarchical clustering and correlation analysis were combined to compare with the result from functional and causal connectivity in previous study.

2.4 Result

2.4.1 Behavioral data and group-level activations

There were significant differences in mean reaction times between “go” trials (mean±SD, 963 ± 74 ms, range: 836-1092 ms) and “switch” trials (mean±SD, 1120 ± 87 ms, range: 948-1350 ms; $p<0.0001$). For “go,” “stop,” and “switch” trials, mean accuracy was 0.890 (SD: 0.117) and 0.853 (SD: 0.165), respectively. The mean SSRT was 454 ms (range: 304-737 ms, SD: 96 ms). The results from the previous study revealed the activations associated with proactive inhibition were significant in the visual cortex, the DLPFC, the caudate, the SMA, the IFG, the STN and the M1 of both hemisphere by the conjunction of all successful “go”, “stop” and “switch” trials. Meanwhile, the significant activations were found in the right IFG, the left SMA, the left M1, as well as bilateral activation of STN. (Zhang, F., and Iwaki, S., 2019)

2.4.2 Dynamical causal modeling

I used DCM12 (Friston et al., 2003) to analyze the effective connectivity between the brain regions with significant activations in proactive and reactive inhibition. The optimal architecture of the model compared by Bayesian model selection(BMS) with fixed-effect analysis(FFX) revealed that the effective connectivity from the right IFG to the left SMA was modulated by reactive modulatory effects, and

the effective connection from the left caudate to the right IFG was modulated by proactive modulatory control. I also found the indirect DLPFC-caudate-IFG-SMA-STN-M1 pathway is involved in the implementation of proactive inhibition, while the "shorter" pathway IFG-SMA-STN-M1 involved in the reactive inhibition.

2.4.3 DTI data

The similarity between the white matter tracts in fronto-basal ganglia circuit displayed as a dendrogram showed there are 3 significant clusters (Fig. 13). The first linkage exists between two pathways (IFG-SMA and IFG-STN), which represents the most similarity compared to 6 association pathways. The further clustering analysis revealed the cluster including DLPFC-caudate/caudate-IFG/caudate-STN. The white matter tract SMA-STN has the most dissimilarity compared to other pathways.

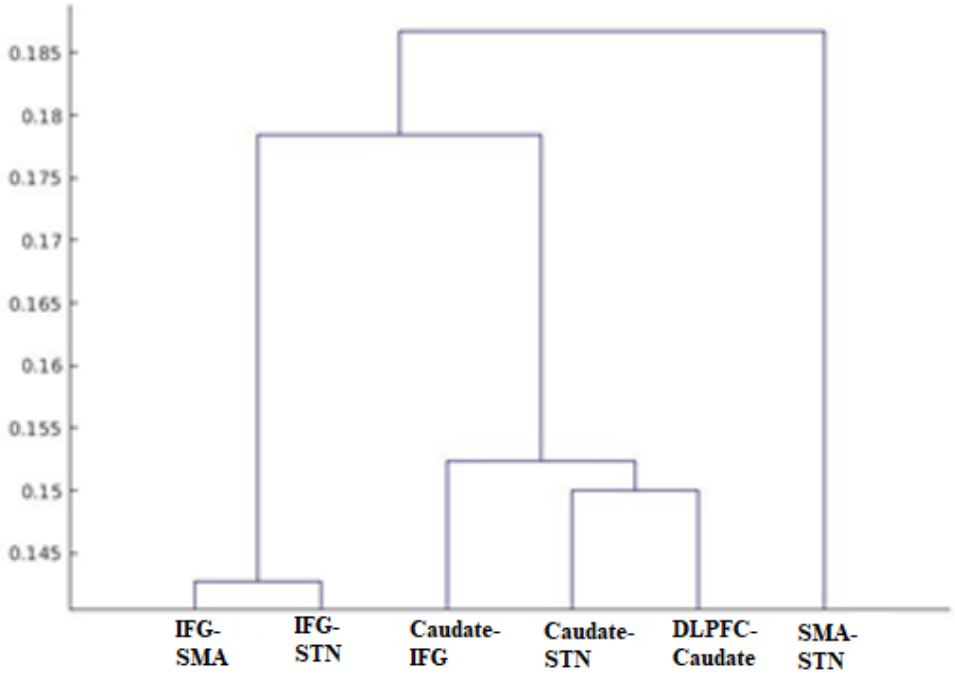

Fig.13. Hierarchical clustering of FA displayed as a dendrogram.

I then calculated the correlations between these tracts with the Spearman's rank correlation coefficient (Fig.14.). The significant correlations were found between the following tracts ($p<0.05$): DLPFC-caudate/caudate-IFG (0.8843), caudate-IFG/IFG-SMA(0.6536), IFG-SMA/SMA-STN(0.8249), IFG-SMA/caudate-STN (0.7933), IFG-SMA/IFG-STN (0.6330), SMA-STN/caudate-STN (0.7481), SMA-STN/IFG-STN(0.6700), caudate-STN/IFG-STN(0.8046).

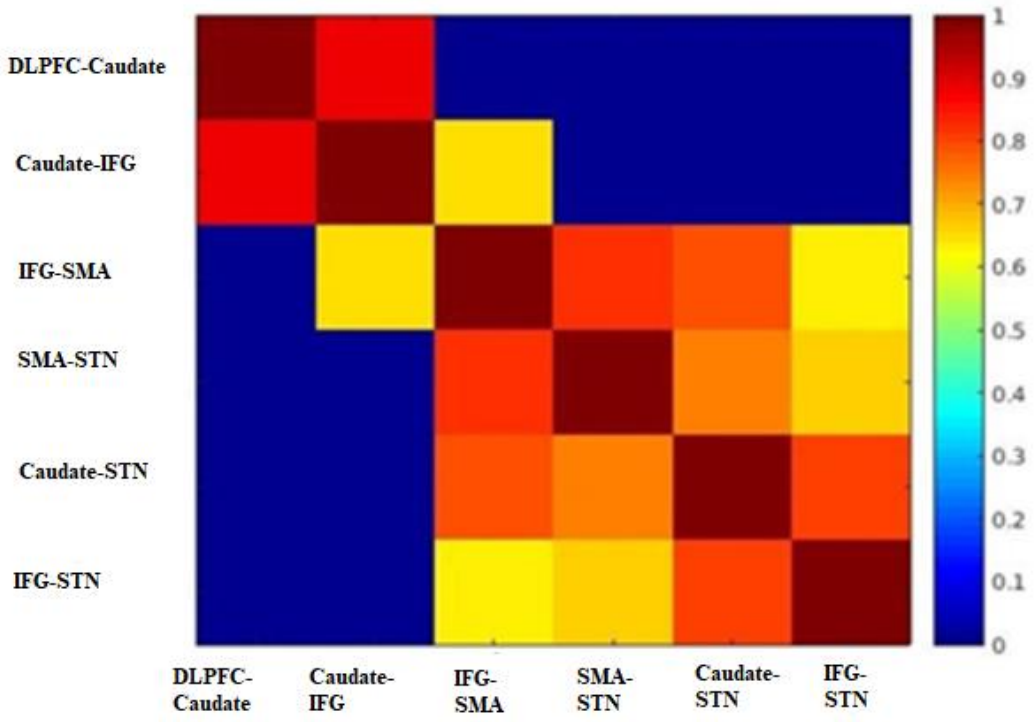

Fig.14. Heat map of interact correlation matrices obtained from tract-level FA.

Matrices for the Spearman's rank correlation coefficient for FA is given in Table 1. All the correlation coefficient was positive.

Table 1

Matrix of Spearman's rank correlation coefficient for FA between white matter tracts of intertest:

	DLPFC-Caudate	Caudate-IFG	IFG-SMA	SMA-STN	Caudate-STN	IFG-STN
DLPFC-Caudate	1	0.8843	0	0	0	0
Caudate-IFG	0.8843	1	0.6536	0	0	0

IFG-SMA	0	0.6536	1	0.8249	0.7933	0.6330
SMA-STN	0	0	0.8249	1	0.7481	0.6700
Caudate-STN	0	0	0.7933	0.7481	1	0.8046
IFG-STN	0	0	0.6330	0.6700	0.8046	1

2.5 Discussion

In the present study, I used a data-driven method to investigate the contribution of local white matter structure to response inhibition function, as well as the relationship between anatomical and functional/effective connectivity. For the first time, I revealed the specific clustering patterns as well as the significant correlations between white matter tracts in the fronto-basal ganglia circuit for response inhibition. Furthermore, I found correspondence between the structural and effective pathways and provide evidence for the existence of hyper-direct and indirect pathways in anatomical networks.

Specific patterns of white matter tracts in the fronto-basal ganglion circuit

The dendrogram showed that strong homology existed in white matter integrity as measured with FA between the DLPFC-caudate/caudate-IFG/caudate-STN, which is in line with the results of previous studies. Comparative tract-tracing studies in monkeys and DTI studies in humans have revealed that the DLPFC is connected with the caudate (Parent, 1990; Parent and Hazrati, 1995;Lehericy et al., 2004) and that the caudate is one of the main basal ganglia nuclei receiving axons from nearly the entire cortex (Maurice et al., 1998; Kolomiets et al., 2001, 2003). Furthermore, studies related to

striatal anatomical and functional connectivity have proven that the caudate is one of the main input nuclei of the basal ganglia and that the rostral/ventral caudate nucleus receives frontal input from the orbital and medial prefrontal cortex (Kunishio and Haber, 1994; Haber et al., 2000; Nakahara et al., 2002). A Transcranial Magnetic Stimulation (TMS) study revealed that stimulation of the DLPFC increased neural activity in the caudate (Strafella et al., 2001; Knoch et al., 2006). A DTI study also found that the head of the caudate was connected to the DLPFC (Lehericy et al., 2004). The DLPFC-caudate circuit was also shown to be involved in selective inhibition via the indirect pathway (Mink, 1996; Jahfari et al., 2011).

The homology between the IFG-SMA/IFG-STN is also supported by the results of previous studies. DTI and more advanced diffusion imaging methods have been used to study the connectivity of the SMA region in humans and have shown the fibers connecting the SMA with the fronto-opercular region (area 44 or “Broca’s area”) (Lehericy et al., 2004; Klein et al., 2007; Oishi et al., 2008; Ford et al., 2010). There is converging evidence that the SMA and IFG play critical roles in controlling inappropriate response tendencies via their connections with the STN (Aron et al., 2007a; Jahfari et al., 2011; Rae et al., 2015). Research on inhibitory control has also provided evidence that the fronto-basal ganglia pathways support motor control via

hyper-direct and indirect pathways; the former bypass the striatum, including the caudate, and directly connect the cortex and STN, and the latter transmit cortical activity to the striatum and then inhibit the activity of the thalamus (Albin et al., 1989; DeLong et al., 1990; Nambu et al., 2000; Mallet et al., 2016).

In the further investigation of microstructural correlations among white matter tracts, I established that the current results indicate that there are statistically significant inter-tract correlations in tract-based measures of FA. In the DLPFC/caudate/IFG/STN cluster (DLPFC-caudate, caudate-IFG, caudate-STN), the most tightly correlated pairs of tracts in term of FA are the DLPFC-caudate/caudate-IFG (0.8843), and no significant correlation was found between the DLPFC-caudate and caudate-STN tracts. In the IFG/SMA/STN cluster (IFG-SMA, IFG-STN), the two tracts with homologous features also showed a significant correlation.

Compared with the results of the hierarchical clustering analysis, I found that many, but not all, of the strong homologous tracts were tightly correlated. However, the presence of significant correlations between two tracts does not signify that they are homologous. For FA values, particularly strong non-homologous correlations were found in the caudate-STN and IFG-SMA.

The FA correlations appear to reflect known functional similarities and differences between tracts, while the value of FA has become the consensus measure of white matter microstructural "integrity" throughout the DTI literature due to its ability to measure the degree of directionality of diffusion within a voxel (Conturo et al., 1999; Basser et al., 2000; Gossl et al., 2002). Thus, the results of the hierarchical clustering and the correlation matrix provided evidence of correspondence between the functional and structural pathways within the fronto-basal ganglion network, although some regions without direct structural connections exhibited strong functional connectivity.

Probabilistic tractography infers the functional pathway

Comparison between the results of the clustering and correlation analyses revealed specific clustering patterns and significant correlations between white matter tracts. Numerous studies involving both humans and non-human primates have concluded that the DLPFC plays a central role in monitoring environmental cues to develop appropriate response strategies (Watanabe, 1990, 1992; Asaad et al., 2000; Ragozzino, 2007; Hikosaka and Isoda, 2010), and the results of the DCM analysis also provided evidence that the DLPFC acts as a driving input during proactive inhibition. Combined with the results of hierarchical clustering that revealed clustering in the DLPFC/caudate/IFG/STN, it is reasonable to consider the DLPFC as the primary region

receiving environmental cues, and then based on the results of the correlation analysis, I found that only the caudate-IFG white matter tract was significantly correlated with the DLPFC-caudate tract. As I continued the investigation of correlations between white matter tracts showing functional similarities, I found that the white matter tracts with significant correlations construct a directional functional pathway: the DLPFC-caudate caudate-IFG/ IFG-SMA/ SMA-STN pathway (Fig. 15.).

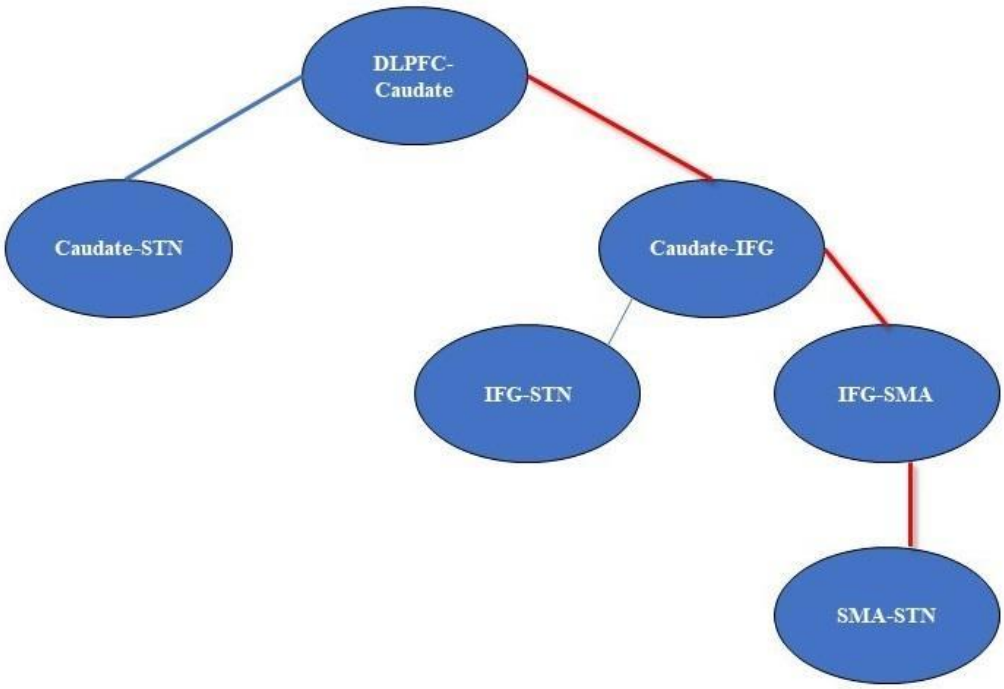

Fig. 15. A "strategy" the behavioral inhibition. DLPFC-Caudate tract acts as the beginning to receive the information, and there is only one possible follow-up with significant correlation: Caudate-IFG. Based on this top-down process, the interact correlations of white matter tracts predict the effective pathways in

response inhibition. SMA: supplementary motor area, STN: subthalamic nucleus, IFG: inferior frontal gyrus, DLPFC: dorsolateral prefrontal cortex.

In previous study, I found that the fronto-basal ganglia pathways are commonly involved in proactive and reactive inhibition, with a "longer" pathway (DLPFC-caudate-IFG-SMA-STN) playing a modulatory role in proactive inhibitory control, and a "shorter" pathway (IFG-SMA-STN) involved in reactive inhibition. In this study, I found that the results of the clustering pattern and correlation analyses for the fronto-basal ganglia circuit are consistent with the previous results of functional and DCM analyses for the fronto-basal ganglia circuit. Furthermore, the separate clusters revealed that the IFG-SMA white matter tract is less homologous compared with the DLPFC-caudate and caudate-IFG white matter tracts, which also supported the existence of two different pathways: the hyperdirect pathway and indirect pathway.

In this study, I did not find a significant correlation between FA and SSRT, although a correlation between SSRT and behavioral data was found in the previous study. I suggest several explanations for this lack of correlation. One possibility is that task performance may be the result of more complex network interactions between structure and function. The results from the hierarchical clustering and correlation

matrix also suggested that there is correspondence between the functional and structural pathways within the fronto-basal ganglion network, although some regions without direct structural connections exhibited strong functional connectivity. The divergence between the structural and functional networks may be attributed to the lack of correlation between structure and task performance. In addition, the tracts identified in the structural network are shared by different functional networks. In this case, some white matter tracts would not be specific for spatial inhibitory control tasks.

2.6 Conclusion

To conclude, the results of the hierarchical clustering and correlation analyses revealed that there is correspondence between the structural and functional pathways in the fronto-basal ganglia circuit. Furthermore, I found that probabilistic tractography can infer the functional and effective pathway in response inhibition.

General discussion

The aim of the dissertation was to investigate the neural mechanism of the generation and control of action. In the first study, I used fMRI data acquired during a stop-signal paradigm task to identify the cortical and subcortical areas involved in proactive and reactive inhibitory processes. To evaluate the modulatory effects of proactive and reactive inhibition on the effective connections between these areas, I first conducted a DCM analysis where 70 DCM models were compared. The results indicate that the increasing activity in effective connectivity from the left SMA to the left STN was modulated by the right IFG, and the decreasing activity in effective connectivity from the right IFG to the left SMA was modulated by both proactive and reactive modulatory effects. I further investigated an alternative hypothesis with 13 additional DCM models in which the causal connection from/to the right DLPFC and the left caudate were considered for proactive inhibition. The results of the additional DCM model comparison show that the increased activity of the effective connection from the left caudate to the right IFG was modulated by proactive modulatory control, which resulted in the inhibitory effects in the connections from the right IFG to the left SMA in the comparison between proactive and reactive inhibitory control. In the second

study, I used a data-driven method to investigate the contribution of local white matter structure to response inhibition function, as well as the relationship between anatomical and functional/effective connectivity. For the first time, I revealed the specific clustering patterns as well as the significant correlations between white matter tracts in the fronto-basal ganglia circuit for response inhibition. Furthermore, I found correspondence between the structural and effective pathways and provide evidence for the existence of hyper-direct and indirect pathways in anatomical networks.

Conclusion

The current dissertation contributes to the neural mechanisms and network for behavioral control. I found that the effective connection from the IFG to the SMA is associated with reactive inhibition, while the effective connection from the caudate to the IFG is associated with proactive inhibition. The indirect DLPFC-caudate-IFG-SMA-STN-M1 pathway is involved in the implementation of proactive modulation, while the hyperdirect pathway that bypasses the striatum contributes to reactive inhibition. The function of the IFG is more related to attention control, and the caudate more likely acts as a "gate" between proactive and reactive inhibition. The hierarchical clustering and correlation analyses further revealed that there is correspondence between the structural and functional pathways in the fronto-basal ganglia circuit. Furthermore, I found that probabilistic tractography can infer the functional and effective pathway in response inhibition.

References

Albin, R. L., Young, A. B., and Penney, J. B. (1989). The functional anatomy of basal ganglia disorders. Trends Neurosci. 12, 366–375.

Alexander, G. E., DeLong, M. R., and Strick, P. L. (1986). Parallel organization of functionally segregated circuits linking basal ganglia and cortex. Annu. Rev. Neurosci. 9, 357–381.

Almgren, H., Van de Steen, F., Kuhn, S., Razi, A., Friston, K., and Marinazzo, D. (2018). Variability and reliability of effective connectivity within the core default mode network: a multi-site longitudinal spectral DCM study. Neuroimage 183, 757–768.

Arfanakis K, Haughton VM, Carew JD, et al. Diffusion tensor MR imaging in diffuse axonal injury. AJNR Am J Neuroradiol. 2002; 23:794–802.

Aron AR. (2011). From reactive to proactive and selective control: developing a richer model for stopping inappropriate responses. Biol Psychiatry 69: e55–68.

Aron, A. R., Behrens, T. E., Smith, S., Frank, M. J., and Poldrack, R. A. (2007a). Triangulating a cognitive control network using diffusion weighted magnetic resonance imaging (MRI) and functional MRI. J. Neurosci. 27, 3743–3752.

Aron, A. R., Durston, S., Eagle, D. M., Logan, G. D., Stinear, C. M., and Stuphorn, V. (2007b). Converging evidence for a fronto-basal ganglia network for inhibitory control of action and cognition. J. Neurosci. 27, 11860–11864.

Aron, A. R., Fletcher, P. C., Bullmore, E. T., Sahakian, B. J., and Robbins, T. W. (2003). Stop-signal inhibition disrupted by damage to right inferior frontal gyrus in humans. Nat. Neurosci. 6, 115-116.

Aron, A. R., and Poldrack, R. A. (2006). Cortical and subcortical contributions to stop signal response inhibition: role of the subthalamic nucleus. J. Neurosci. 26, 2424–2433.

Aron, A. R., Robbins, T., and Poldrack, R. A. (2004). Inhibition and the right inferior frontal cortex. Brain 127, 1561–1573.

Aron, A. R., Robbins, T., and Poldrack, R. A. (2014). Inhibition and the right inferior frontal cortex: one decade on. Trends Cogn. Sci. 18, 177–185.

Arthurs, O. J. & Boniface, S. (2002). How well do we understand the neural origins of the fMRI BOLD signal? Trends in Neurosciences 25(1):27–31.

Assad, W. F., Rainer, G., and Miller, E. K. (1998). Neural activity in the primate prefrontal cortex during associative learning. Neuron 21, 1399–1407.

Asaad W.F., Rainer G, Miller EK. (2000). Task-specific neural activity in the primate prefrontal cortex. J Neurophysiol 84: 451–459.

Ay H, Buonanno FS, Schaefer PW, et al. Posterior leukoencephalopathy without severe hypertension: utility of diffusion-weighted MRI. Neurology. 1998; 51:1369–76.

Baker, K. B., Lee, J. Y., Mavinkurve, G., Russo, G. S., Walter, B., DeLong, M. R., et al. (2010). Somatotopic organization in the internal segment of the globus pallidus in Parkinson's disease. Exp. Neurol. 222, 219–225.

Band, G. P. H., van der Molen, M. W., and Logan, G. D. (2003). Horse-race model simulations of the stop-signal procedure. Acta Psychol. 112, 105–142.

Bannon, S., Gonsalvez, C. J., Croft, R. J. & Boyce, P. M. (2002). Response inhibition deficits in obsessive-compulsive disorder. Journal of Psychiatric Research, 110, 165-174.

Bari, A., and Robbins, T. W. (2013). Inhibition and impulsivity: behavioral and neural basis of response control. Prog. Neurobiol. 108, 44–79.

Barkley, R. A. (1997). Behavioral inhibition, sustained attention, and executive functions: Constructing a unifying theory of ADHD. Psychological Bulletin, 121, 65-94.

Basser PJ, Mattiello J, Le Bihan D. Estimation of the effective self-diffusion-tensor from the NMR spin echo. J Magn Reson B 1994; 103:247–54.

Basser, P.J., Pierpaoli, C., (1996). Microstructural and physiological features of tissues elucidated by quantitative diffusion tensor MRI. J. Magn. Reson. B 111, 209-219.

Basser, P., & Pierpaoli, C. (1996). Microstructural features measured using diffusion tensor imaging. Journal of Magnetic Resonance. Series B, 111(3), 209-219.

Basser, P.J., Pajevic, S., Pierpaoli, C., Duda, J., Aldroubi, A., (2000). In vivo fiber tractography using DT-MRI data. Magn. Reson. Med. 44(4), 625-632.

Behrens, T.E., Johansen-Berg, H., Woolrich, M. W., Smith, S. M., Wheeler-Kingshott, C. A., Boulby, P. A. et al. (2003) Non-invasive mapping of connections between human thalamus and cortex using diffusion imaging. Nat. Neurosci., 6, 750-757.

Benoit, R. G., and Anderson, M. C. (2012). Opposing mechanisms support the voluntary forgetting of unwanted memories. Neuron 76, 450–460.

Braver TS, Gray JR, Burgess G.C. (2007). Explaining the many varieties of working memory variation: dual mechanisms of cognitive control. In Variation in working memory (ed. Conway A, et al.), pp. 76–106. Oxford University Press, Oxford.

Brett, M., Johnsrude, I. S., and Owen, A. M. (2002). The problem of functional localization in the human brain. Nat. Rev. Neurosci. 3, 243–249.

Brunberg J, Chenevert T, McKeever P, et al. In vivo MR determination of water diffusion coefficients and diffusion anisotropy: correlation with structural alteration in gliomas of the cerebral hemispheres. AJNR Am J Neuroradiol. 1995; 16:361–71.

Bryden, D. W., Burton, A. C., Kashtelyan, V., Barnett, B. R., and Roesch, M. R. (2012). Response inhibition signals and miscoding of direction in dorsomedial striatum. Front. Integr. Neurosci. 6:69.

Bunge, S. A., Dudukovic, N. M., Thomason, M. E., Vaidya, C. J., and Gabrieli, J. D. (2002). Immature frontal lobe contributions to cognitive control in children: evidence from fMRI. Neuron 33, 301–311.

Cai, Y., Li, S., Liu, J., Li, D., Feng, Z., Wang, Q., et al. (2016). The role of the frontal and parietal cortex in proactive and reactive inhibitory control: a transcranial direct current stimulation study. J. Cogn. Neurosci. 28, 177–186.

Cai, W., Oldenkamp, C., and Aron, A. R. (2011). A proactive mechanism for selective suppression of response tendencies. J. Neurosci. 31, 5965–5969.

Casey, B., Epstein, J., Buhle, J., Liston, C., Davidson, M., Tonev, S., et al (2007) Frontostriatal connectivity and its role in cognitive control in parent-child dyads with ADHD. Am. J. Psychiatry 164, 1729-1736.

Chambers, C. D., Bellgrove, M. A., Stokes, M. G., and Henderson, T. R. (2006). Executive “brake failure” following deactivation of human frontal lobe. J. Cogn. Neurosci. 18, 444–455.

Chambers, C. D., Garavan, H., and Bellgrove, M. A. (2009). Insights into the neural basis of response inhibition from cognitive and clinical neuroscience. Neurosci. Biobehav. Rev. 33, 631–646.

Chevalier, N., Kurth, S., Doucette, M.R., Wiseheart, M., Deoni, SCL., Dean, D.C., O’Muircheartaigh, J., Blackwell, KA., Munakata, Y., LeBourgeois, MK., (2015) Myelination Is Associated with Processing Speed in Early Childhood: Preliminary Insights. PLoS ONE 10: e0139897.

Chevalier N, Kurth S, Doucette MR, Wiseheart M, Deoni SCL, Dean DC, O’Muircheartaigh J, Blackwell KA, Munakata Y, LeBourgeois MK (2015) Myelination Is Associated with Processing Speed in Early Childhood: Preliminary Insights Huang H, ed. PLOS One 10: e0139897.

Chikazoe, J. (2010). Localizing performance of go/no-go tasks to prefrontal cortical subregions. Curr. Opin. Psychiatry 23, 267–272.

Chikazoe, J., Jimura, K., Asari, T., Yamashita, K., Morimoto, H., Hirose, S., et al. (2009a). Functional dissociation in right inferior frontal cortex during performance of a go/no-go task. Cereb. Cortex 19, 146–152.

Chikazoe, J., Jimura, K., Hirose, S., Yamashita, K., Miyashita, Y., and Konishi, S. (2009b). Preparation to inhibit a response complements response inhibition during performance of a stop-signal task. J. Neurosci. 29, 15870–15877.

Chien D, Kwong KK, Gress DR, et al. MR diffusion imaging of cerebral infarction in humans. AJNR Am J Neuroradiol 1992; 13:1097–102, discussion 1103–05.

Chikazoe, J., Jimura, K., Hirose, S., Yamashita, K., Miyashita, Y., and Konishi, S. (2009b). Preparation to inhibit a response complements response inhibition during performance of a stop-signal task. J. Neurosci. 29, 15870–15877.

Chikazoe, J. (2010). Localizing performance of go/no-go tasks to prefrontal cortical subregions. Curr. Opin. Psychiatry 23, 267–272.

Chopra, S., Shaw, M., Shaw, T., Sachdev, PS., Anstey, KJ., Cherbuin, N., (2018). More highly myelinated white matter tracts are associated with faster processing speed in healthy adults. NeuroImage 171: 332-340.

Cohen, J. D., Barch, D. M., Carter, C., and Servan-Schreiber, D. (1999). Context-processing deficits in schizophrenia: converging evidence from three theoretically motivated cognitive tasks. J. Abnorm. Phychol. 108, 120–133.

Conturo, T.E., Lori, N.F., Cull, T.S., Akbudak, E., Snyder, A.Z., Shimony, J.S., McKinstry, R.C., Burton, H., Raichle, M.E. (1999) Tracking neuronal fiber pathways in the living human brain. Proc. Natl. Acad. Sci. U.S.A. 96(18), 10422-10427.

Corbetta, M., and Shulman, G. L. (2002). Control of goal-directed and stimulus driven attention in the brain. Nat. Rev. Neurosci. 3, 201–215.

Coxon, J. P., Stinear, C. M., and Byblow, W. D. (2006). Intracortical inhibition during volitional inhibition of prepared action. J. Neurophysiol. 95, 3371–3383.

Criaud, M., Wardak, C., Ben Hamed, S., Ballanger, B., and Boulinguez, P. (2012). Proactive inhibitory control of response as the default state of executive control. Front. Psychol. 3:59.

Cunillera, T., Fuentemilla, L., Brignani, D., Cucurell, D., and Miniussi, C. (2014). A simultaneous modulation of reactive and proactive inhibition processes by anodal tDCS on the right inferior frontal cortex. PLoS One 9: e113537.

Daunizeau, J., David, O., and Stephan, K. E. (2011). Dynamic causal modelling: a critical review of the biophysical and statistical foundations. Neuroimage 58, 312–322.

DeLong, M. R. (1990). Primate models of movement disorders of basal ganglia origin. Trends Neurosci. 13, 281–285.

D.J. Werring, C.A. Clark, G.J. Parker, D.H. Miller, A.J. Thompson, G.J. Barker. (1999) A direct demonstration of both structure and function in the visual system: combining diffusion tensor imaging with functional magnetic resonance imaging, Neuroimage 9, 352-361.

Dunovan, K., Lynch, B., Molesworth, T., and Verstynen, T. (2015). Competing basal ganglia pathways determine the difference between stopping and deciding not to go. Elife 4: e08723.

Eagle, D. M., Bari, A., and Robbins, T. W. (2008). The neuropsychopharmacology of action inhibition: cross species translation of the stop-signal and go/no-go tasks. Psychopharmacology 199, 439–456.

Eagle, D.M., Baunez, C., Hutcheson, D.M., Lehmann, O., Shah, A.P., Robbins, T.W., 2008. Stop-signal reaction-time task performance: role of prefrontal cortex and subthalamic nucleus. Cereb. Cortex 18, 178-188.

Ebisu T, Naruse S, Horikawa Y, et al. Discrimination between different types of white matter edema with diffusion-weighted MR imaging. J Magn Reson Imaging 1993; 3:863–68.

Ebisu T, Tanaka C, Umeda M, et al. Discrimination of brain abscess from necrotic or cystic tumors by diffusion-weighted echo planar imaging. Magn Reson Imaging 1996; 14:1113–16.

Erika-Florence, M., Leech, R., and Hampshire, A. (2014). A functional network perspective on response inhibition and attentional control. Nat. Commun. 5:4073.

Felleman, D., Van Essen, D.C., 1991. Distributed hierarchical processing in the primate cerebral cortex. Cereb. Cortex 1, 1–47.

Fields, RD (2008). White matter in learning, cognition and psychiatric disorders. Trends Neurosci 31: 361-370

Ford, A., McGregor, K.M., Case, K., et al. (2010) Structural connectivity of Broca's area and medial front cortex. Neuroimage 52: 1230-7.

Forstmann, B. U., Keuken, M. C., Jahfari, S., Bazin, P. L., Neumann, J., Schaafer, A., et al. (2012). Cortico-subthalamic white matter tract strength predicts interindividual efficacy in stopping a motor response. Neuroimage 60, 370–375.

Frank, M. J., Samanta, J., Moustafa, A. A., and Sherman, S. J. (2007). Hold your horses: impulsivity, deep brain stimulation and medication in parkinsonism. Science 318, 1309–1312.

Friston, K. J., Harrison, L., Penny, W. (2003) Dynamic causal modelling. NeuroImage 19: 1273-1302.

Friston , K. et al.(2017). Dynamic causal modelling revisited. Neuroimage Published online February 17,2017.

Gonzalez RG, Schaefer PW, Buonanno FS, et al. Diffusion-weighted MR imaging: diagnostic accuracy in patients imaged within 6 hours of stroke symptom onset. Radiology 1999; 210:155–62.

Gossl, C., Fahrmeir, L., Putz, B., Auer, L.M., Auer, D.P., (2002) Fiber tracking from DTI using linear state space models: detectablity of the pyramidal tract. Neuroimage 16(2), 378-388.

Haber, S.N., Fudge, J.L., McFarland, N.R., (2000). Striatonigrostriatal pathways in primates from an ascending spiral from the shell to the dorsolateral striatum. J. Neurosci. 20, 2369-2382.

Hamani, C., Saint-Cyr, J. A., Fraser, J., Kaplitt, M., and Lozano, A. M. (2004). The subthalamic nucleus in the context of movement disorders. Brain 127, 4–20.

Hampshire, A., Chamberlain, S. R., Monti, M. M., Duncan, J., and Owen, A. M. (2010). The role of the right inferior frontal gyrus: inhibition and attentional control. Neuroimage 50, 1313–1319.

Hampshire, A. (2015). Putting the brakes on inhibitory models of frontal lobe function. Neuroimage 113, 340–355.

Hardman, C., Henderson, J. M., Finkelstein, D. I., Horne, M. K., Paxinos, G., and Halliday, G. M. (2002). Comparison of the basal ganglia in rats, marmosets, macaques, baboons and humans: volume and neuronal number for the output, internal relay and striatal modulating nuclei. J. Comp. Neurol. 445, 238–255.

Harnishfeger, K. K. & Björklund, D. F. (1994). A developmental perspective on individual differences in inhibition. Learning and Individual Differences, 6, 331-355

Hazrati, L. N., and Parent, A. (1992). The striatopallidal projection displays a high degree of anatomical specificity in the primate. Brain Res. 592, 213–227.

Hergan K, Schaefer PW, Sorensen AG, et al. Diffusion-weighted MRI in diffuse axonal injury of the brain. Eur Radiol 2002; 12:2536–41.

Hikosaka, O., and Isoda, M. (2010). Switching from automatic to controlled behavior: cortico-basal ganglia mechanisms. Trends Cogn. Sci. 14, 154–161.

Hilgetag, C.C., O'Neill, M.A., Young, M.P., 2000. Hierarchical organization of macaque and cat cortical sensory systems explored with a novel network processor. Philos. Trans. R. Soc. B: Biol. Sci. 355, 71–89.

Honey, C.J., Thivierge, J.P., Van Impe, A., Geurts, M., Van Hecke, W., Sunaert, S., Wenderoth, N., Swinnen, S.P. (2012). Can structure predict function in the human brain? Neuroimage 52, 766-776.

Huettel, S. A., Song, A. W. and McCarthy, G. (2008) Functional Magnetic Resonance Imaging. Second Edi. Sinauer Associates.

Huisman TA, Sorensen AG, Hergan K, et al. Diffusion-weighted imaging for the evaluation of diffuse axonal injury in closed head injury.

Jaffard M, Benraiss A, Longcamp M, Velay JL, Boulinguez P. (2007). Cueing method biases in visual detection studies. Brain Res 1179: 106–118.

Jaffard, M., Longcamp, M., Velay, J.-L., Anton, J.-L., Roth, M., Nazarian, B., et al. (2008). Proactive inhibitory control of movement assessed by event-related fMRI. Neuroimage 42, 1196–1206.

Jahfari, S., Stinear, C. M., Claffey, M., Verbruggen, F., and Aron, A. R. (2010). Responding with restraint: what are the neurocognitive mechanisms? J. Cogn. Neurosci. 22, 1479–1492.

Jahfari, S., Verbruggen, F., Frank, M. J., Waldorp, L. J., Colzato, L., Ridderinkhof, K. R., et al. (2012). How preparation changes the need for top-down control of the basal ganglia when inhibiting premature actions. J. Neurosci. 32, 10870–10878.

Jahfari S, Waldorp L, van den Wildenberg WP, Scholte HS, Ridderinkhof KR, Forstmann BU (2011) Effective connectivity reveals important roles for both the hyperdirect (fronto-subthalamic) and the indirect (frontostriatal-pallidal) fronto-basal ganglia pathways during response inhibition. J Neurosci 31:6891–6899.

Kenner, N. M., Mumford, J. A., Hommer, R. E., Skup, M., Leibenluft, E., and Poldrack, R. A. (2010). Inhibitory motor control in response stopping and response switching. J. Neurosci. 30, 8512–8518.

Kim Y, Chang K, Kim H, et al. Brain abscess and necrotic or cystic brain tumor: discrimination with signal intensity on diffusion-weighted MR imaging. AJR Am J Roentgenol 1998; 171:1487–90.

King, A. V., Linke, J., Gass, A., Hennerici, M. G., Tost, H., Poupon, C., & Wessa, M. l. (2012). Microstructure of a three-way anatomical network predicts individual differences in response inhibition: a tractography study. Neuroimage, 59(2), 1949-1959.

Klein, J.C., Behrens, T.E., Robson, M.D., et al. (2007) Connectivity-based parcellation of human cortex using diffusion MRI: Establishing reproducibility, validity and observer independence in BA 44/45 and SMA/pre-SMA. Neuroimage 34, 204-11.

Klingberg, T., Hedegus, M., Temple, E., Salz, T., Gabrieli, J.D., Moseley, M.E., Poldrack, R.A. (2000) Microstructure of temporo-parietal white matter as a basis for reading ability: evidence from diffusion tensor magnetic resonance imaging. Neuron 25, 493-500.

Kolomies, B.P., Deniau, J.M., Glowinski, J., Thierry, A.M. (2003) Basal ganglia and processing of cortical information: functional interactions between trans-striatal and trans-subthalamic circuits in the substantia nigra pars reticulata. Neuroscience 117: 931-938.

Kolomies, B.P., Deniau, J.M., Mailly, P., Menetrey, A., Glowinski, J., Thierry, A.M. (2001) Segregation and convergence of information flow through the cortico-subthalamic pathways. J Neurosci 21: 5764-5772.

Knoch, D., Treyer, V., Regard, M., Muri, R.M., Buck, A., Weber, B. (2006) Lateralized and frequency-dependent effects of prefrontal rTMS on regional cerebral blood flow. Neuroimage 31, 641-648.

Krabbe K, Gideon P, Wagn P, et al. MR diffusion imaging of human intracranial tumours. Neuroradiology 1997; 39:483–89.

Kubicki, M., Westin, C. F., Marier, S. E., Mamata, H., Frumin, M., Ersner-Hershfried, H. et al. (2002) Diffusion tensor imaging and its appication to neurophychiatric disorders. Harv. Rev. Psychiatry, 10, 324-336.

Kunishio, K., Haber, S.N., (1994) Primte cingulostriatal projection: limbic striatal versus sensorimotor striatal input. J. Comp. Neurol. 350,337-356.

Lappin, J.S., Eriksen, C.W., (1966). Use of a delayed signal to stop a visual reaction-time response. J. Exp. Psychol. 72, 805–811.

Lehéricy, S., Ducros, M., Van de Moortele, P. F., Francois, C., Thivard, L., Poupon, C., et al. (2004). Diffusion tensor fiber tracking shows distinct corticostriatal circuits in humans. Ann. Neurol. 55, 522–529.

Leuthardt EC, Wippold FJ 2nd, Oswood MC, et al. Diffusion-weighted MR imaging in the preoperative assessment of brain abscesses. Surg Neurol 2002; 58:395–402.

Liston, C., Watts, R., Tottenham, N., Davidson, M. C., Niogi, S., Ulug, A.M., et al (2006) Frontostriatal microstructure modulates efficient recruitment of cognitive control. Cerebral Cortex 16, 553-560.

Lehericy S, Ducros M, Van de Moortele PF, Francois C, Thivard L, Poupon C, Swindale N, Ugurbil K, Kim DS. (2004). Diffusion tensor fiber tracking shows distinct corticostriatal circuits in humans. Ann Neurol 55: 522–529.

Lehericy, S., Ducros, M., Krainik, A., et al. (2004) 3-D diffusion tensor axonal tracking shows distinct SMA and pre-SMA projections to the human striatum. Cereb Cortex 14: 1302-9.

Logan, G. D., and Cowan, W. B. (1984). On the ability to inhibit thought and action: a theory of an act of control. Psychol. Rev. 91, 295–327.

Logan, G.D., Cowan, W.B., Davis, K.A., (1984). On the ability to inhibit simple and choice reaction time responses: a model and a method. J. Exp. Psychol. 10, 276– 291.

Logan, G., Schachar, R., and Tannock, R. (1997). Impulsivity and inhibitory control. Psychol. Sci. 8, 60–64.

Majid, D. S., Cai, W., Corey-Bloom, J., and Aron, A. R. (2013). Proactive selective response suppression is implemented via the basal ganglia. J. Neurosci. 33, 13259–13269.

Mallet, N., Schmidt, R., Leventhal, D., Chen, F., Amer, N., Boraud, T., et al. (2016). Arkypallidal cells send a stop signal to striatum. Neuron 89, 308–316.

Mancini, C., Cardona, F., Baglioni, V., Panunzi, S., Pantano, P., Suppa, A., et al. (2018). Inhibition is impaired in children with obsessive-compulsive symptoms but not in those with tics. Mov. Disord. 33, 950–959.

Mancini, C., Modugno, N., Santilli, M., Pavone, L., Grillea, G., Morace, R., et al. (2019). Unilateral stimulation of subthalamic nucleus does not affect inhibitory control. Front. Neurol. 9:1149.

Mattia, M., Pani, P., Mirabella, G., Costa, S., Del Giudice, P., and Ferraina, S. (2013). Heterogeneous attractor cell assemblies for motor planning in premotor cortex. J. Neurosci. 33, 11155–11168.

Mattia, M., Spadacenta, S., Pavone, L., Quarato, P., Esposito, V., Sparano, A., et al. (2012). Stop-event-related potentials from intracranial electrodes reveal a key role of premotor and motor cortices in stopping ongoing movements. Front. Neuroeng. 5:12.

Maurice, N., Deniau, J.M., Glowinski, J., Thierry, A.M. (1998) Relationships between the prefrontal cortex and the basal ganglia in the rat: physiology of the corticosubthalamic circuits. J Neurosci 18: 9539-9546.

Mallet, N., Schmidt, R., Leventhal, D., Chen, F., Amer, N., Boraud, T., et al. (2016). Arkypallidal cells send a stop signal to striatum. Neuron 89, 308–316.

Marks MP, De Crespigny A, Lentz D, et al. Acute and chronic stroke: navigated spin-echo diffusion-weighted MR imaging. Radiology 1996; 199:403–08.

Maurice N, Deniau JM, Glowinski J, Thierry AM (1998) Relationships between prefrontal cortex and the basal ganglia in the rat: physiology of the cortico subthalamic circuits. J Neurosci 18: 9539-9546.

McLoughlin, G., Albrecht, B., Banaschewski, T., Rothenberger, A., Brandeis, D., Asherson, P. & Kuntsi, J. (2010). Electrophysiological evidence for abnormal preparatory states and inhibitory processing in adult ADHD. Behavioral and Brain Functions, 6, 1-12.

Mink JW. (1996). The basal ganglia: focused selection and inhibition of competing motor programs. Prog Neurobiol 50: 381–425.

Mirabella, G. (2014). Should I stay or should I go? Conceptual underpinnings of goal-directed actions. Front. Syst. Neurosci. 8:206.

Mirabella, G., Fragola, M., Giannini, G., Modugno, N., and Lakens, D. (2017). Inhibitory control is not lateralized in Parkinson's patients. Neuropsychologia 102, 177–189.

Mirabella, G., Iaconelli, S., Modugno, N., Giannini, G., Lena, F., and Cantore, G. (2013). Stimulation of subthalamic nuclei restores a near normal planning strategy in Parkinson's patients. PLoS One 8: e62793.

Mirabella, G., Iaconelli, S., Romanelli, P., Modugno, N., Lena, F., Manfredi, M., et al. (2012a). Deep brain stimulation of subthalamic nuclei affects arm response inhibition in Parkinson's patients. Cereb. Cortex 22, 1124–1323.

Mirabella, G., Iaconelli, S., Spadacenta, S., Federico, P., and Gallese, V. (2012b). Processing of hand related verbs specifically affects the planning and execution of arm reaching movements. PLoS One 7: e35403.

Mirabella, G., Pani, P., and Ferraina, S. (2008). Context influences on the preparation and execution of reaching movements. Cogn. Neuropsychol. 25, 996–1010.

Mirabella, G., Pani, P., and Ferraina, S. (2011). Neural correlates of cognitive control of reaching movements in the dorsal premotor cortex of rhesus monkeys. J. Neurophysiol. 106, 1454–1466.

Mori S, Kaufmann WE, Pearlson GD, et al. Three-dimensional tracking of axonal projections in the brain by magnetic resonance imaging. Ann Neurol 1999; 45:265–69.

Moseley ME, Cohen Y, Mintorovitch J, et al. Early detection of regional cerebral ischemia in cats: comparison of diffusion- and T2-weighted MRI and spectroscopy. *Magn Reson Med* 1990; 14:330–46.

Mukherjee, P., McKinstry RC. Reversible posterior leukoencephalopathy syndrome: evaluation with diffusion-tensor MR imaging. Radiology 2001; 219:756–65.

Mukherjee, P., Berman, J. I., Chung, S. W., Hess, C. P., Henry, R. G., (2008) "Diffusion tensor MR imaging and fiber tractography: theoretic underpinnings.," AJNR. American journal of neuroradiology, vol. 29, no. 4, pp. 632-41.

Nakahara, K., Hayashi, T., Konishi, S., Miyashita, Y., (2002) Functional MRI of macaque monkeys performing a cognitive set-shifting task. Science 295, 1532-1536.

Nambu, A., Tokuno, H., Hamada, I., Kita, H., Imanishi, M., Akazawa, T., et al. (2000). Excitatory cortical inputs to pallidal neurons via the subthalamic nucleus in the monkey. J. Neurophysiol. 84, 289–300.

Nambu, A., Tokuno, H., and Takada, M. (2002). Functional significance of the cortico-subthalamo-pallidal 'hyperdirect' pathway. Neurosci. Res. 43, 111–117.

Niogi, S.N., Mukherjee, P., Ghajar, J., Johnson, C.E., Kolster, R., Lee, H., Suh, M., Zimmerman, R.D., Manley, G.T., McCandliss, B.D. (2008b) Structural dissociation of attentional control and memory in adults with and without mild traumatic brain injury. Brain 131,3209-3221.

Oishi, K., Zilles, K., Amunts, K., et al. (2008) Human brain white matter atlas: identification and assignment of common anatomical structures in superficial white matter. Neuroimage 43: 447-57.

Pajevic, S., and Pierpaoli, C. (1999) Color schemes to represent the orientation of anisotropic tissues from diffusion tensor data: application to white matter fiber tract mapping in the human brain. Magn Reson. Med., 42, 526-540.

Parent A. (1990). Extrinsic connections of the basal ganglia. Trends Neurosci. 13: 254–258.

Parent A, Hazrati LN. (1995). Functional anatomy of the basal ganglia. I. The cortico-basal ganglia-thalamo-cortical loop. Brain Res Rev 20: 91–127.

Penny, W. D., Stephan, K. E., Mechelli, A., and Friston, K. J. (2004). Comparing dynamic causal models. Neuroimage 22, 1157–1172.

Pierpaoli, C., Jezzard, P., Basser, P.J., Barnett, A., Di Chiro, G. (1996) Diffusion tensor MR imaging of the human brain. Radiology 201, 637-648.

Provenzale JM, Petrella JR, Cruz LCH Jr, et al. Quantitative assessment of diffusion abnormalities in posterior reversible encephalopathy syndrome. AJNR Am J Neuroradiol. 2001; 22:1455–61.

Rae, C. L., Hughes, L. E., Anderson, M. C., and Rowe, J. B. (2015). The prefrontal cortex achieves inhibitory control by facilitating subcortical motor pathway connectivity. J. Neurosci. 35, 786–794.

Ragozzino ME. (2007). The contribution of the medial prefrontal cortex, orbitofrontal cortex, and dorsomedial striatum to behavioral flexibility. Ann N Y Acad Sci 1121: 355–375.

Schwartz R, Mulkern R, Gudbjartsson H, et al. Diffusion-weighted MR imaging in hypertensive encephalopathy: clues to pathogenesis. AJNR Am J Neuroradiol 1998; 19:859–62.

Seidl A. H. (2014), Regulation of conduction time along axons. Neuroscience 276: 126 -134.

Servan-Schreiber, D., Cohen, J., and Steingard, S. (1996). Schizophrenic deficits in processing of cortex: a test of a theoretical model. Arch. Gen. Psychiatry 53, 1105–1112.

Sharp, D.J., Bonnelle, V., de Boissezon, X., Beckmann, C.F., James, S.G., Patel, M.C., Mehta, M.A., (2010). Distinct frontal systems for response inhibition, attentional capture, and error processing. Proc. Natl. Acad. Sci. U. S. A. 107,6106 - 6111.

Simmonds, D. J., Pekar, J. J., and Mostofsky, S. H. (2008). Meta-analysis of go/no-go tasks demonstrating that fMRI activation associated with response inhibition is task dependent. Neuropsychologia 46, 224–232.

Smith JS, Cha S, Mayo MC, et al. Serial diffusion-weighted magnetic resonance imaging in cases of glioma: distinguishing tumor recurrence from postresection injury. J Neurosurg 2005; 103:428–38.

Smittenaar, P., Guitart-Masip, M., Lutti, A., and Dolan, R. J. (2013). Preparing for selective inhibition within frontostriatal loops. J. Neurosci. 33, 18087–18097.

Strafella, A.P., Paus, T., Barrett, J., Dagher, A. (2001) Repetitive transcranial magnetic stimulation of the human prefrontal cortex induces dopamine release in the caudate nucleus. J. Neurosci. 21, RC157.

Stroop, J.R. (1935) Studies of interference in serial verbal reactions. Journal of Experimental Psychology, 28, 643–662.

Swann, N. C., Cai, W., Conner, C. R., Pieters, T. A., Claffy, M. P., Georges, J. S., et al. (2012). Roles for the pre-supplementary motor area and the right inferior frontal gyrus in stopping action: electrophysiological responses and functional and structural connectivity. Neuroimage 59, 2860–2870.

Thomson, A.M., Bannister, A.P., 2003. Interlaminar connections in the neocortex. Cereb. Cortex 13, 5–14.

Thomsen C, Henriksen O, Ring P. In vivo measurement of water self-diffusion in the human brain by magnetic resonance imaging. Acta Radiol 1987; 28:353–61.

Tien R, Felseberg G, Friedman H, et al. MR imaging of high-grade cerebral gliomas: value of diffusion-weighted echoplanar pulse sequences. AJR Am J Roentgenol 1994; 162:671–77.

Tzourio-Mazoyer, N., Landeau, B., Papathanassiou, D., Crivello, F., Etard, O., Delcroix, N., et al. (2002). Automated anatomical labeling of activations in SPM using a macroscopic anatomical parcellation of the MNI MRI single-subject brain. Neuroimage 15, 273–289.

van Belle, J., Vink, M., Durston, S., and Zandbelt, B. B. (2014). Common and unique neural networks for proactive and reactive response inhibition revealed by independent component analysis of functional MRI data. Neuroimage 103, 65–74.

van den Wildenberg, W. P., van Boxtel, G. J., van der Molen, M. W., Bosch, D. A., Speelman, J. D., and Brunia, C. H. (2006). Stimulation of the subthalamic region facilitates the selection and inhibition of motor responses in Parkinson's disease. J. Cogn. Neurosci. 18, 626–636.

van Rooij, S. J. H., Geuze, E., Kennis, M, Rademaker, A. R. & Vink, M. (2014). Neural Correlates of Inhibition and Contextual Cue Processing Related to Treatment Response in PTSD. Neuropsychopharmacology, 40, 667–675

Verbruggen, F., and Logan, G. D. (2008). Automatic and controlled response inhibition: associative learning in the go/no-go and stop-signal paradigms. J. Exp. Psychol. Gen. 137, 649–672.

Verbruggen, F., and Logan, G. D. (2009). Proactive adjustments of response strategies in the stop-signal paradigm. J. Exp. Psychol. Hum. Percept. Perform. 35, 835–854.

Verbruggen, F., Stevens, T., and Chambers, C. D. (2014). Proactive and reactive stopping when distracted: an attentional account. J. Exp. Psychol. Hum. Percept. Perform. 40, 1295–1300.

Warach S, Chien D, Li W, et al. Fast magnetic resonance diffusion-weighted imaging of acute human stroke. Neurology 1992; 42:1717–23. Erratum in: Neurology 1992; 42:2192.

Wardak, C. (2011). The role of the supplementary motor area in inhibitory control in monkeys and humans. J. Neurosci. 31, 5181–5183.

Watanabe M. (1990). Prefrontal unit activity during associative learning in the monkey. Exp Brain Res 80: 296–309.

Watanabe M. (1992). Frontal units of the monkey coding the associative significance of visual and auditory stimuli. Exp Brain Res 89: 233–247.

Zhang, F., and Iwaki, S. (2019). Common Neural Network for Different Functions: An Investigation of Proactive and Reactive Inhibition. Front. Behav. Neurosci., 13:124.